AMERICAN SOCIETY FOR MICROBIOLOGY | Journal of Virology

New Member of the V1V2-Directed CAP256-VRC26 Lineage That Shows Increased Breadth and Exceptional Potency

Nicole A. Doria-Rose,[a] Jinal N. Bhiman,[b,c] Ryan S. Roark,[a] Chaim A. Schramm,[d] Jason Gorman,[a] Gwo-Yu Chuang,[a] Marie Pancera,[a] Evan M. Cale,[a] Michael J. Ernandes,[a] Mark K. Louder,[a] Mangaiarkarasi Asokan,[a] Robert T. Bailer,[a] Aliaksandr Druz,[a] Isabella R. Fraschilla,[a] Nigel J. Garrett,[e] Marissa Jarosinski,[a] Rebecca M. Lynch,[a] Krisha McKee,[a] Sijy O'Dell,[a] Amarendra Pegu,[a] Stephen D. Schmidt,[a] Ryan P. Staupe,[a] Matthew S. Sutton,[a] Keyun Wang,[a] Constantinos Kurt Wibmer,[b,c] Barton F. Haynes,[f] Salim Abdool-Karim,[e,g] Lawrence Shapiro,[d] Peter D. Kwong,[a] Penny L. Moore,[b,c,e] Lynn Morris,[b,c,e] John R. Mascola[a]

Vaccine Research Center, National Institute of Allergy and Infectious Diseases, National Institutes of Health, Bethesda, Maryland, USA[a]; Centre for HIV and STIs, National Institute for Communicable Diseases of the National Health Laboratory Services, Johannesburg, South Africa[b]; University of the Witwatersrand, Johannesburg, South Africa[c]; Department of Biochemistry and Systems Biology, Columbia University, New York, New York, USA[d]; Centre for the AIDS Programme of Research in South Africa (CAPRISA), University of KwaZulu Natal, Durban, South Africa[e]; Duke University School of Medicine and Center for HIV/AIDS Vaccine Immunology-Immunogen Discovery at Duke University, Durham, North Carolina, USA[f]; Department of Epidemiology, Columbia University, New York, New York, USA[g]

ABSTRACT

The epitopes defined by HIV-1 broadly neutralizing antibodies (bNAbs) are valuable templates for vaccine design, and studies of the immunological development of these antibodies are providing insights for vaccination strategies. In addition, the most potent and broadly reactive of these bNAbs have potential for clinical use. We previously described a family of 12 V1V2-directed neutralizing antibodies, CAP256-VRC26, isolated from an HIV-1 clade C-infected donor at years 1, 2, and 4 of infection (N. A. Doria-Rose et al., Nature 509:55–62, 2014, http://dx.doi.org/10.1038/nature13036). Here, we report on the isolation and characterization of new members of the family mostly obtained at time points of peak serum neutralization breadth and potency. Thirteen antibodies were isolated from B cell culture, and eight were isolated using trimeric envelope probes for differential single B cell sorting. One of the new antibodies displayed a 10-fold greater neutralization potency than previously published lineage members. This antibody, CAP256-VRC26.25, neutralized 57% of diverse clade viral isolates and 70% of clade C isolates with remarkable potency. Among the viruses neutralized, the median 50% inhibitory concentration was 0.001 μg/ml. All 33 lineage members targeted a quaternary epitope focused on V2. While all known bNAbs targeting the V1V2 region interact with the N160 glycan, the CAP256-VRC26 antibodies showed an inverse correlation of neutralization potency with dependence on this glycan. Overall, our results highlight the ongoing evolution within a single antibody lineage and describe more potent and broadly neutralizing members with potential clinical utility, particularly in areas where clade C is prevalent.

IMPORTANCE

Studies of HIV-1 broadly neutralizing antibodies (bNAbs) provide valuable information for vaccine design, and the most potent and broadly reactive of these bNAbs have potential for clinical use. We previously described a family of V1V2-directed neutralizing antibodies from an HIV-1 clade C-infected donor. Here, we report on the isolation and characterization of new members of the family mostly obtained at time points of peak serum neutralization breadth and potency. One of the new antibodies, CAP256-VRC26.25, displayed a 10-fold greater neutralization potency than previously described lineage members. It neutralized 57% of diverse clade viral isolates and 70% of clade C isolates with remarkable potency: the median 50% inhibitory concentration was 0.001 μg/ml. Our results highlight the ongoing evolution within a single antibody lineage and describe more potent and broadly neutralizing members with potential clinical utility, particularly in areas where clade C is prevalent.

Neutralizing antibodies (NAbs) against HIV-1 are likely to be a major component of an effective vaccine-induced immune response. Cross-reactive NAbs commonly arise during HIV-1 infection, though only a small subset of infected patients produces NAbs with a high neutralization breadth and potency (1–4). In contrast, the HIV-1 envelope glycoprotein (Env) vaccine immunogens tested to date have failed to elicit cross-reactive neutralizing antibodies (5, 6). Thus, studying the development of broadly neutralizing antibodies (bNAbs) in infected individuals may provide important lessons for vaccine design (5, 7–10). In addition, the isolation of bNAbs from selected donors has greatly aided our understanding of the HIV-1 Env structure (11–13) and vulnerability to neutralizing antibodies (14–16), and such antibodies have the potential to be used for the prevention or treatment of HIV-1 infection (8, 17).

NAbs directed to the V1V2 region of HIV-1 Env are of particular interest for vaccine design, as this site is antigenic and commonly targeted in HIV infection (18, 19). To date, families of V1V2-directed bNAbs have been isolated from only four different donors (20–23). These antibodies typically have a long, anionic heavy chain complementarity-determining region 3 (CDRH3), which penetrates the glycan shield, and heavy chain variable (VH) gene mutation levels of 10 to 20%. They bind to the apex region of the intact trimer and bind poorly or not at all to most monomeric forms of the protein. Negative-stain electron microscopy studies show that such antibodies bind with a stoichiometry of one per trimer and likely interact with more than one protomer (21, 24), consistent with the location of V1V2 at the apex of the trimer (11, 12). This category of antibodies typically relies on glycan residues, specifically, N156 and N160 in V2 (23). Glycan dependence some-

times results in incomplete neutralization, referred to as the plateau effect (23, 25, 26), due in part to the microheterogeneity of glycoforms at these residues, resulting in a resistant subpopulation within a virus preparation (27).

Our group has extensively studied the antibodies from donor CAP256, who developed high-titer plasma neutralizing antibodies to the V1V2 region that first appeared at 1 year and peaked at 3 years of HIV-1 infection (21, 28, 29). This donor was infected with a clade C virus and 15 weeks later was superinfected with a different clade C virus. We isolated 12 V1V2-directed antibodies at multiple time points over 4 years of infection; all were somatically related and termed the CAP256-VRC26 lineage, where CAP256 denotes the donor and VRC26 denotes the antibody lineage. Members of this antibody lineage have a very long CDRH3 of 35 to 37 amino acids and modest levels of V-gene mutation (8 to 15% sequence divergence compared with that of the germ line). 454 pyrosequencing of virus from early time points showed that the long CDRH3 was present at the origin of the lineage and allowed accurate inference of an unmutated common ancestor (UCA) that was able to bind and neutralize the superinfecting virus (21).

Here, we report on the isolation and characterization of 21 new members of the CAP256-VRC26 family. These antibodies were isolated either by B cell culture or by single-cell sorting with trimeric Env probes. One of the antibodies, CAP256-VRC26.25 (where the antibody name indicates donor-lineage.clone), neutralizes 57% of HIV-1 isolates, including 70% of clade C isolates, with an overall 10-fold greater potency than the previously described family members. Structure, epitope mapping, and phylogenetic analyses provide a deeper understanding of the origin and evolution of this important lineage.

MATERIALS AND METHODS

Study subject. Centre for the AIDS Programme of Research in South Africa (CAPRISA) participant CAP256 was enrolled into the CAPRISA Acute Infection Study (30) that was established in 2004 in KwaZulu-Natal, South Africa, for follow-up and subsequent identification of HIV seroconversion. CAP256 was one of the seven women in this cohort who developed neutralization breadth (31). The CAPRISA 002 Acute Infection Study was reviewed and approved by the research ethics committees of the University of KwaZulu-Natal (E013/04), the University of Cape Town (025/2004), and the University of the Witwatersrand (MM040202). CAP256 provided written informed consent for study participation. Samples were drawn between 2005 and 2009.

B cell cultures. Peripheral blood mononuclear cells (PBMCs) isolated from CAP256 blood draws at week 193 were stained with LIVE/DEAD Fixable Aqua (Invitrogen), CD19-Cy7-phycoerythrin (PE), IgM-Cy5-PE, IgD-PE, CD16-Pacific Blue, and CD3-Cy7-allophycocyanin (APC) (BD Pharmingen). The IgD-negative (IgD^-) IgM-negative (IgM^-) B cells were bulk sorted on a BD FACSAria II flow cytometer as described previously (19). Cells were plated at 2 B cells per well in 384-well plates and cultured for 14 days in the presence of CD40L-expressing irradiated feeder cells, interleukin-2 (IL-2) (Roche), and interleukin-21 (IL-21) (Gibco), as described previously (32, 33). Culture supernatants were screened by microneutralization against HIV-1 ZM53.12 and CAP210.E8 Env pseudoviruses as described in reference 34.

Expression and purification of trimeric HIV-1 Env BG505 SOSIP.664 probes. An Avi tag (GLNDIFEAQKIEWHE) was inserted at the C terminus of the previously described construct BG505 SOSIP.664.T332N gp140, referred to here as BG505 SOSIP (35). For BG505 SOSIP.K169E-Avi, lysine (K) 169 was mutated to a glutamic acid (E) by site-directed mutagenesis. Both constructs were transfected and purified as described previously (12). Briefly, HEK 293 cells were cotransfected with BG505 SOSIP and furin plasmid DNAs at a 4:1 ratio. Transfection supernatants were harvested and purified through either a VRC01 or a 2G12 antibody affinity column. Proteins were eluted with 3 M $MgCl_2$, 10 mM Tris, pH 8.0. The eluate was concentrated and applied to a Superdex 200 column equilibrated in 5 mM HEPES, pH 7.5, 150 mM NaCl, 0.02% azide or phosphate-buffered saline. The fractions corresponding to the trimeric proteins were pooled, concentrated, flash-frozen in liquid nitrogen, and stored at −80°C. The proteins were biotinylated at the Avi tag sequence using BirA ligase and then conjugated to streptavidin-APC or streptavidin-PE (Invitrogen) as described previously (36).

The probes were assessed for the correct antigenicity by binding to antibody-coated beads. Anti-mouse kappa light chain beads (Becton Dickinson, San Jose, CA) were incubated with anti-human IgG (Becton Dickinson), washed, incubated with 2 μg/ml antibody CAP256-VRC26.09, PGT128, or F105, and washed again. BG505 SOSIP-streptavidin-APC or BG505 SOSIP.K169E-streptavidin-PE (1.5 μg) was then incubated with the beads, and the beads were washed and analyzed on an LSR II flow cytometer (Becton Dickinson).

Cell sorting. PBMCs from week 159 were stained for IgG-positive (IgG^+) B cells using LIVE/DEAD Fixable Aqua (Invitrogen), IgG-fluorescein isothiocyanate, CD19-Cy7-PE, IgM-Cy5-PE, CD14-PE-Texas Red (ECD), CD4-ECD, CD3-Cy7-APC, and CD8-Brilliant Violet 711 (BD Pharmingen). At the same time, they were stained with BG505 SOSIP-streptavidin-APC and BG505 SOSIP.K169E-streptavidin-PE. Cells that were BG505 SOSIP-streptavidin-APC positive (APC^+) IgG^+ $CD19^+$ were sorted using a BD FACSAria II flow cytometer into single wells of a 96-well plate containing RNase inhibitor (New England Biolabs), SuperScript reverse transcriptase buffer (Invitrogen), dithiothreitol, and Igepal as described previously (36).

Isolation and expression of CAP256-VRC26 family genes. Kappa and lambda light chain gene and IgG heavy chain gene variable regions were amplified from neutralization-positive B cell culture wells as described in reference 33 or from 96-well sort plates as described in reference 36. Briefly, cells were lysed and subjected to reverse transcription-PCR (RT-PCR) as described in reference 37 using a modified primer set (see Table S1 in the supplemental material). These primers were developed by our group or were described previously (see Table S1 in the supplemental material) (37–39). Briefly, cells were lysed and subjected to RT-PCR as described previously (37) using a modified primer and a round of nested PCR with 3 different multiplex primer pools, which were used to amplify either the heavy chains or the light chains. The amplicons were subcloned, expressed, and purified as described in reference 19. For antibodies CAP256-VRC26.13 to CAP256-VRC26.21, wells that previously yielded VRC26-lineage lambda chains but no heavy chains were subjected to RT-PCR using IgA-specific 3′ primers. All heavy chains were subcloned and expressed as IgG1 regardless of the class of the original amplicon.

Neutralization assays. Single-round-of-replication Env pseudoviruses were prepared, titers were determined, and the pseudoviruses were

Received 31 July 2015 Accepted 21 September 2015
Accepted manuscript posted online 14 October 2015
Citation Doria-Rose NA, Bhiman JN, Roark RS, Schramm CA, Gorman J, Chuang G-Y, Pancera M, Cale EM, Ernandes MJ, Louder MK, Asokan M, Bailer RT, Druz A, Fraschilla IR, Garrett NJ, Jarosinski M, Lynch RM, McKee K, O'Dell S, Pegu A, Schmidt SD, Staupe RP, Sutton MS, Wang K, Wibmer CK, Haynes BF, Abdool-Karim S, Shapiro L, Kwong PD, Moore PL, Morris L, Mascola JR. 2016. New member of the V1V2-directed CAP256-VRC26 lineage that shows increased breadth and exceptional potency. J Virol 90:76–91. doi:10.1128/JVI.01791-15.
Editor: G. Silvestri
Address correspondence to John R. Mascola, jmascola@nih.gov.
Supplemental material for this article may be found at http://dx.doi.org/10.1128/JVI.01791-15.

used to infect TZM-bl target cells as described previously (40, 41). The neutralization breadth of CAP256-VRC26.25, CAP256-VRC26.26, and CAP256-VRC26.27, as well as that of previously described antibodies, was determined using a previously described panel (19, 36) of up to 200 geographically and genetically diverse Env pseudoviruses representing the major subtypes and circulating recombinant forms. The remaining CAP256-VRC26 antibodies were assayed on a 46-virus subset of this panel, along with the autologous virus strains CAP256.2.00.C7J (a primary infecting [PI] strain) and CAP256.206.c9 (a superinfecting [SU] strain). The data were calculated as a reduction in the number of luminescence units compared with the number for the control wells and are reported as the 50% inhibitory concentration (IC_{50}; in micrograms per microliter) for monoclonal antibodies (MAbs).

N160 glycan mutant Env pseudoviruses were generated by site-directed mutagenesis as described previously (28, 42). All N160 glycan mutants had the N160K mutation, except for ConC, which had the N160A mutation. The N156 mutants (this study) were generated as N156A mutants by site-directed mutagenesis (GeneImmune, New York, NY). The BG505 pseudovirus had the wild-type sequence (threonine) at position 332, unlike the BG505 SOSIP probe, which bears a T332N mutation (35).

Neutralization and autoreactivity data for CAP256-VRC26.25 were generated with a variant that had the amino acid change K126Q in the light chain, which was inserted during subcloning. We confirmed that this single amino acid change did not alter the neutralization data.

Autoreactivity. CAP256-VRC26.01 to CAP256-VRC26.32 and UCA antibodies were assayed at 25 and 50 $\mu g\ ml^{-1}$ for autoreactivity to HEp-2 cells (Inverness Medical Professional Diagnostics) by indirect immunofluorescence and for binding to cardiolipin as described previously using a Quanta Lite ACA IgG III assay (INOVA Diagnostics Inc., San Diego, CA) (43). The UCA and seven of the antibodies with the broadest activity were further evaluated on a panel of autoantigens using an AtheNA Multi-Lyte ANA-II Plus test system (Alere, Orlando, FL) to detect semiquantitatively IgG antibodies to 9 separate analytes, SSA, SSB, Sm, RNP, Scl-70, Jo-1, centromere B, double-stranded DNA (dsDNA), and histone, as reported previously (43); values of >120 at 25 $\mu g\ ml^{-1}$ were considered positive (43).

Next-generation sequencing analysis. 454 pyrosequencing was performed on PBMCs from week 34, the results for which are reported here, as well as PBMCs from weeks 38, 49, 59, 119, 176, and 206, the results for which were described previously (21). mRNA was prepared from 10 million to 15 million PBMCs as follows: cells were lysed in 600 μl buffer RLT (Qiagen) per 10 million PBMCs and run over a QIAshredder (Qiagen). The flowthrough was applied to the DNA column from an Allprep kit (Qiagen), and that flowthrough was used for subsequent purification using an Oligotex kit (Qiagen). cDNA was synthesized using SuperScript II reverse transcriptase (Invitrogen) and oligo$(dT)_{12–18}$ primers with incubation at 70°C for 1 min, chilling on ice, and then synthesis at 42°C for 2 h. Individual PCRs were performed with Phusion polymerase (Thermo) for 30 cycles. Primers (21) consisted of pools of 5 to 7 oligonucleotides specific for all lambda chain gene families or for VH3 family genes and had adapters for 454 next-generation sequencing. For PBMCs from week 176 only, heavy chain PCR was performed with primers for all VH families and mixed lambda chain and kappa chain primers were used for the light chain (21). PCR products were gel purified (Qiagen). Pyrosequencing of the PCR products was performed on a GSFLX sequencing instrument (Roche-454 Life Sciences, Bradford, CT, USA) on a half chip per reaction (full chips were used for PBMCs from week 176). On average, ~250,000 raw reads were produced.

Next-generation sequencing data from each time point were processed through an Antibodyomics pipeline (https://github.com/scharch/SONAR) as previously described (21, 44). Briefly, a series of Python scripts was used to check transcripts for appropriate length (300 to 600 nucleotides), provide calls for germ line V and J gene assignments by BLAST analysis, and check for in-frame junctions and open reading frames. Reads for which the V and J genes were successfully assigned and that had an in-frame junction and no stop codons were clustered using the CDHit program (45) at 97.25% identity, and singletons were discarded. In order to better account for possible errors introduced during sequencing, we restricted our analysis to sequences appearing at least twice in any one data set. This resulted in approximately 50% fewer final heavy chain sequences than we previously reported, but the phylogenetic structure of the lineage remained the same. In addition, we used a CDRH3 signature contained in all previously reported sequences as a less computationally intensive way of finding related heavy chain sequences. Thus, heavy chain sequences that matched the CAP256-VRC26 VH and JH assignments and that had CDRH3s that were at least 30 amino acids long and that had a YY motif were selected and combined across all time points. Light chains that matched the CAP256-VRC26 VL and JL assignments and that had a light chain complementarity-determining region 3 (CDRL3) with at least 92% sequence identity to a known CAP256-VRC26 family member were manually inspected, and those with a recombination pattern matching that of the known antibodies were combined across all time points. Selected heavy and light chains from all time points were reclustered so that sequences observed at multiple time points are represented only once in the final data set. A final manual inspection was used to remove sequences with apparent PCR crossover or homopolymer indel errors.

Heavy and light chain trees were built using the FASTML program (46), and the light chain tree was manually edited to match the heavy chain arrangement as previously described (21). Ancestral sequences were inferred from these trees using the DNAML program (47) as previously described (21).

CAP256-VRC26.25 Fab crystallization and structure determination. Fab was prepared by inserting an HRV3C recognition site (GLEVL FQGP) after Lys 235. Purified IgG was incubated with HRV3C protease overnight at 4°C, and the digested protein was passed over protein A agarose to remove the Fc fragment and subsequently purified over a Superdex 200 gel filtration column. The Fab preparation was then screened against 576 crystallization conditions using a Mosquito crystallization robot. Initial crystals were grown by the vapor diffusion method in sitting drops at 20°C by mixing 0.1 μl of protein with 0.1 μl of reservoir solution. Crystals were manually reproduced in hanging drops by mixing 1.0 μl protein complex with 1.0 μl reservoir solution. Crystals grown in a reservoir solution of 23% polyethylene glycol (PEG) 8000 and 0.1 M HEPES, pH 7.5, were flash frozen in liquid nitrogen with 20% PEG 400 as a cryoprotectant. Diffraction data were collected at a wavelength of 1.00 Å at the SER-CAT beamline ID-22 (Advanced Photon Source, Argonne National Laboratory). All diffraction data were processed with the HKL2000 suite (48), and model building and refinement were performed in the COOT (49) and PHENIX (50) programs, respectively. Ribbon diagram representations of protein crystal structures were made with the PyMOL program (51), and electrostatics were calculated and rendered with the UCSF Chimera program (52). Data collection and refinement statistics are shown in Table S2 in the supplemental material.

Amino acid frequency analysis. The resistance score for a given amino acid (or a gap) was defined as the ratio of its number of occurrences in sequences from resistant strains to its overall number of occurrences for the given residue position (53). A higher score indicates that the amino acid was preferentially found among sequences from resistant strains, with a score of 1 indicating that the amino acid was found only among sequences from resistant strains. Associations were analyzed using Fisher's exact test with the Bonferroni correction for multiple comparisons. Alignments were generated using the MUSCLE algorithm implemented in Geneious software, version 8.1.7 (54). Logo plots were generated with the Weblogo application (http://weblogo.berkeley.edu/) (55) and manually colored by the use of Inkscape software (https://inkscape.org).

Accession numbers. Sequences from this study are available in GenBank under the following accession numbers: for the heavy and light chain sequences for CAP256-VRC26.13 to CAP256-VRC26.33, GenBank accession numbers KT371076 to KT371117; for 454 pyrosequencing data

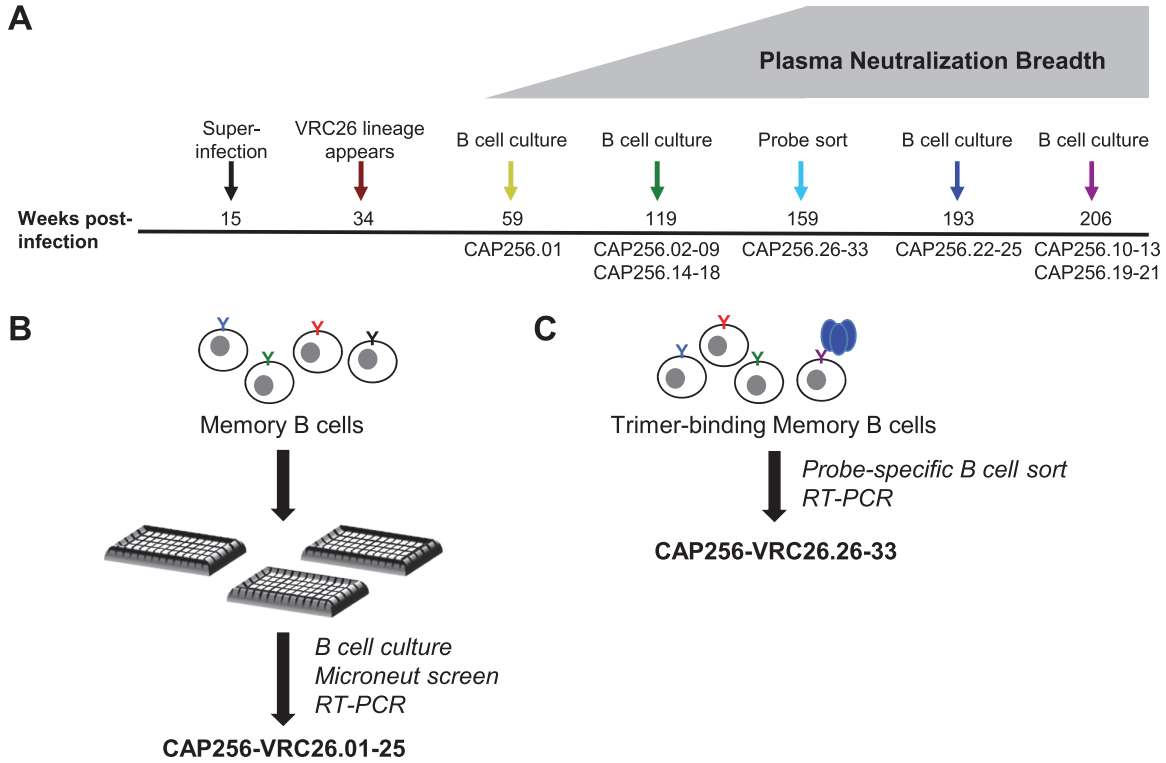

FIG 1 Schematics of CAP256-VRC26 antibody isolation. (A) Timeline of antibody isolation. Numbers above the line indicate the week postinfection. The names of the antibodies isolated at each time point are shown below the line. (B) Schematic of high-throughput B cell culture method. Sorted IgD^- IgM^- B cells were plated at a density of ~2 cells per well into 384-well plates, followed by assessment by a microneutralization assay (Microneut) on day 14. (C) Schematic of probe sorting method. IgG^+ B cells bound to APC-labeled BG505 SOSIP were sorted into 96-well plates, followed by reverse transcription-PCR to recover the IgG genes.

sets from CAP256 at week 34, Sequence Read Archive accession numbers SRR2126754 and SRR2126755; and for pyrosequencing data sets of bioinformatically identified lineage members from week 34, GenBank accession numbers KT371118 to KT371320. Coordinates and structure factors for CAP256-VRC26.25 have been deposited with the Protein Data Bank (PDB) under accession number 5DT1.

RESULTS

Isolation of new antibodies. To further understand the CAP256-VRC26 lineage and in an attempt to find broader and more potent members, we isolated antibodies from time points of peak serum neutralization potency and breadth (Fig. 1A). We used several methods to isolate an additional 21 antibodies. These included repeated PCR amplifications with cDNA from wells from the original B cell cultures, using the new primers described below; a B cell culture of PBMCs from week 193 (Fig. 1B); and single-cell sorting with antigen-specific probes (Fig. 1C), using a PBMC sample from week 159 (at the peak of neutralization breadth in plasma [28, 29]). The recovered antibodies are named as follows: donor-lineage.clone, for example, CAP256-VRC26.25. For brevity, in some figures we refer to them as donor.clone, for example, CAP256.25.

(i) B cell cultures. The B cell culture method used here involves sorting of IgM^- IgD^- B cells, followed by culture for 2 weeks and then microneutralization assays of culture supernatants (32, 34) (Fig. 1B). Previous B cell cultures from donor CAP256 (21) yielded multiple wells from which VRC26-lineage lambda chains, but not IgG heavy chains, were recovered. We used IgA-specific 3′ primers (39) with new sets of multiplex 5′ primers (see Materials and Methods and Table S1 in the supplemental material) and recovered nine VRC26-lineage heavy chains from these wells. Some of these may have derived from IgA^+ B cells, as IgA^+ B cells were not excluded in the sorting. Unexpectedly, two wells yielded both IgG and IgA amplicons with identical variable regions but distinct constant regions (Fig. 2A). We concluded that class switching had occurred in the well during the 2-week culture. The combination of CD40L and IL-21 was previously shown to support IgG-to-IgA class switching in human B cells (56–58). We therefore made the assumption that all such wells originally contained IgG^+ B cells. All antibody sequences were subcloned and expressed as IgG1. This strategy yielded 9 antibodies (CAP256-VRC26.13 to CAP256-VRC26.21) derived from the PBMCs from weeks 119 and 206. We subsequently performed a B cell culture with B cells derived from week 193 and, using the new primer sets described in the Materials and Methods and Table S1 in the supplemental material, recovered four additional antibodies (CAP256-VRC26.22 to CAP256-VRC26.25).

(ii) Single-cell sort with trimer probes. The recent development of the trimer mimic BG505 SOSIP (35) provides a probe that can be used to sort B cells expressing antibodies to quaternary epitopes (59). The broader antibodies of the CAP256-VRC26 lineage neutralize BG505, and thus, we chose to use this probe with the goal of isolating lineage members with broader neutralization capacities (Fig. 1C). To increase the specificity of the probe for the CAP256-VRC26 lineage, we assessed potential mutations that

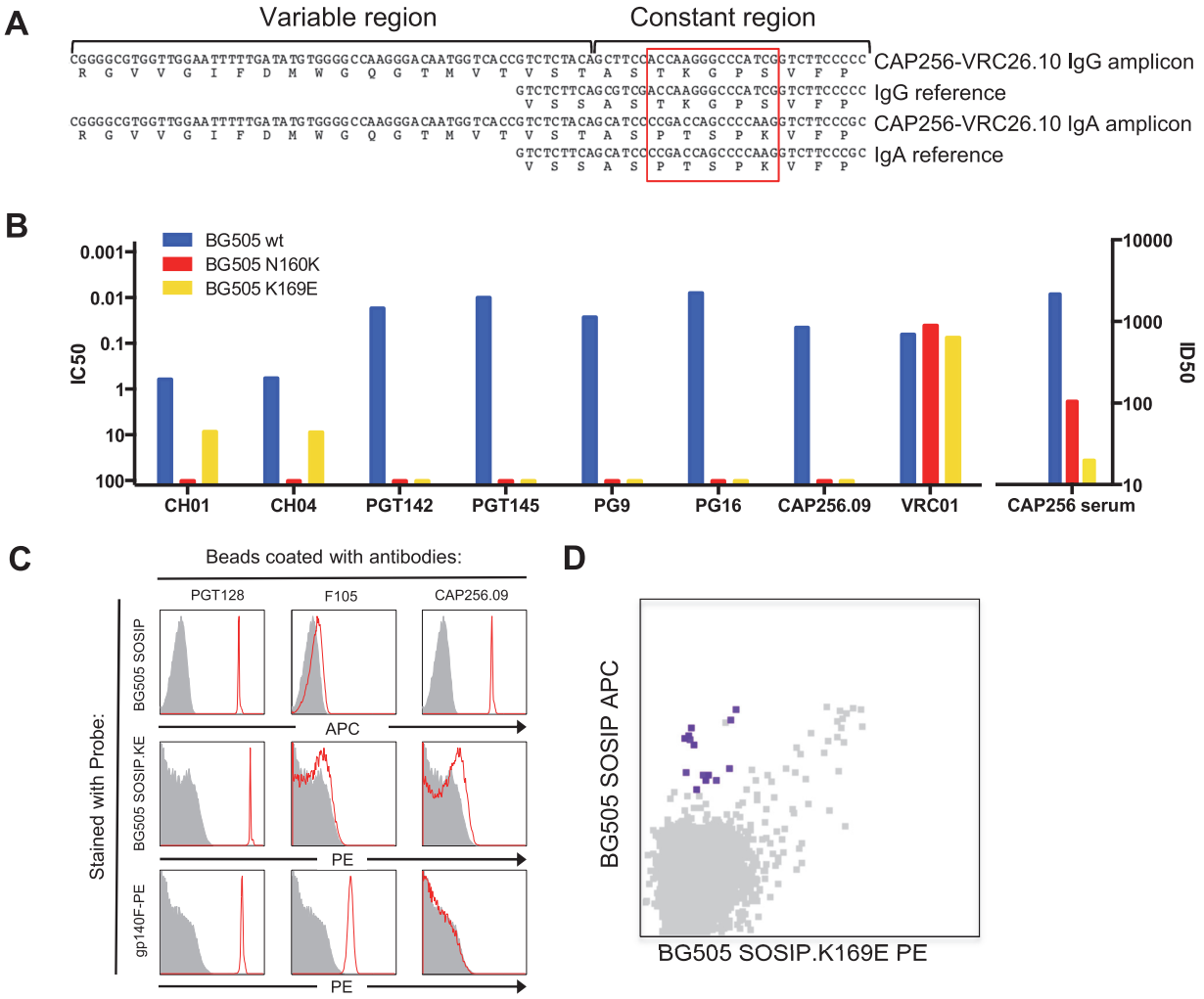

FIG 2 Isolation of CAP256-VRC26 antibodies. (A) Class switch occurs under B cell culture conditions. Identical VDJ regions appear in both IgA and IgG forms in the same well. The red box highlights sequences that differ between IgG and IgA. (B to D) The BG505 trimer with a mutation in V2 selects for CAP256-VRC26-lineage B cells. (B) Effect of N160K and K169E mutations on neutralization of HIV BG505 by V1V2-directed antibodies and CAP256 plasma. wt, wild type; ID50, 50% inhibitory dilution. (C) Quality and specificity of probes. BG505 SOSIP-APC, BG505 SOSIP.K169E-PE, or gp140F-PE probes were used to stain beads coated with the PGT128, F105, or CAP256-VRC26.09 (CAP256.09) antibody. Histograms of anti-HIV antibodies (red) are overlaid on those for the anti-influenza virus control (gray). (D) Probe-specific B cell sorting. CAP256 PBMCs were stained with B cell markers and probes. Sorted IgG^+ BG505 SOSIP-APC^+ BG505-SOSIP-K169E-PE^- B cells (purple) are shown overlaid on all live, IgG^+ B cells (gray).

would knock out V1V2 antibody binding and neutralization: using an Env pseudovirus of BG505, we made a variant with a deletion of the N160 glycan (the N160K mutant) and a variant with a mutation in V2 strand C (the K169E mutant). While the N160K mutation rendered BG505 resistant to PG9-, CH01-, and PGT145-lineage antibodies, neutralization by CAP256 plasma and CAP256-VRC26.09 was more affected by the K169E mutation than by the N160K mutation (Fig. 2B). We therefore made a K169E mutation in the BG505 SOSIP trimer. Wild-type and mutant molecules were fluorescently labeled, and their antigenicity was assessed by binding them to beads coated with known antibodies (Fig. 2C). The BG505 SOSIP wild-type probe bound strongly to PGT128 and CAP256-VRC26.09 and did not bind to the weakly neutralizing antibody F105. The K169E mutant had similar binding, but as expected, it did not bind to CAP256-VRC26.09. As a control, YU2-gp140-foldon, which does not present quaternary epitopes (60, 61), was observed to bind PGT128 and F105 but not CAP256-VRC26.09 (Fig. 2C). Using the BG505 SOSIP probe pair, we sorted single IgG^+ B cells from week 159 (Fig. 2D), a time point at which the donor's plasma showed peak neutralization breadth and potency (28, 29). We amplified and subcloned Ig genes from cells that were positive for the wild-type probe but did not bind the K169E probe. Fourteen wells yielded heavy chain amplicons, light chain amplicons, or both. In 11 of the 14 wells, the amplicon(s) matched the VRC26 lineage, and 8 such wells yielded heavy chain-light chain pairs. All eight pairs were expressed and had neutralizing activity, thus producing lineage members CAP256-VRC26.26 to CAP256-VRC26.33.

Characteristics of the new CAP256-VRC26 antibodies. The 21 new CAP256-VRC26 antibodies showed a range in the levels of nucleotide mutations from the sequences of the germ line genes: mutations in 4.2 to 18% of the nucleotides compared with the sequences of the VH3-30*18 alleles and 2.5 to 15% of the nucleotides compared with the sequences of the VL1-51*02 alleles

TABLE 1 Genetic and neutralization characteristics of CAP256-VRC26 antibodies[a]

Source (wk, isolation method)	Antibody name	% mutation from the sequence of the following allele:		CDRH3 length (no. of amino acids)	Neutralization of 46 strains	
		VH3-30*18	VL1-51*02		% neutralization breadth	Median IC_{50} (μg/ml)
Wk 59, culture	*CAP256-VRC26.01*	*8.3*	*3.9*	*35*	*20*	*3.32*
Wk 119, culture	*CAP256-VRC26.02*	*8.7*	*4.9*	*35*	*17*	*0.44*
	CAP256-VRC26.03	*8.7*	*7.4*	*35*	*35*	*0.06*
	CAP256-VRC26.04	*9.0*	*8.1*	*35*	*30*	*0.27*
	CAP256-VRC26.05	*10*	*5.6*	*35*	*22*	*0.02*
	CAP256-VRC26.06	*11*	*7.4*	*36*	*17*	*0.69*
	CAP256-VRC26.07	*12*	*7.7*	*35*	*13*	*5.00*
	CAP256-VRC26.08	*12*	*9.8*	*37*	*46*	*0.08*
	CAP256-VRC26.09	*14*	*9.8*	*37*	*46*	*0.02*
Wk 206, culture	*CAP256-VRC26.10*	*12*	*3.9*	*35*	*24*	*0.35*
	CAP256-VRC26.11	*13*	*14*	*35*	*26*	*1.04*
	CAP256-VRC26.12	*15*	*8.4*	*35*	*7*	*0.21*
	CAP256-VRC26.13	**15**	**9.5**	**35**	**7**	**0.09**
Wk 119, culture	**CAP256-VRC26.14**	**10**	**7.7**	**35**	**24**	**0.75**
	CAP256-VRC26.15	**10**	**6.7**	**35**	**33**	**0.34**
	CAP256-VRC26.16	**10**	**7.7**	**35**	**28**	**0.67**
	CAP256-VRC26.17	**12**	**8.1**	**35**	**28**	**0.14**
	CAP256-VRC26.18	**12**	**7.4**	**35**	**26**	**1.66**
Wk 206, culture	**CAP256-VRC26.19**	**13**	**10**	**35**	**46**	**0.16**
	CAP256-VRC26.20	**16**	**13**	**37**	**2**	**1.87**
	CAP256-VRC26.21	**18**	**14**	**37**	**13**	**0.58**
Wk 193, culture	**CAP256-VRC26.22**	**16**	**13**	**37**	**46**	**0.04**
	CAP256-VRC26.23	**9.7**	**6.3**	**35**	**7**	**0.03**
	CAP256-VRC26.24	**4.2**	**2.5**	**35**	**7**	**0.46**
	CAP256-VRC26.25	**12**	**9.8**	**36**	**63**	**0.003**
Wk 159, sorting with new probes	**CAP256-VRC26.26**	**17**	**9.8**	**37**	**59**	**0.05**
	CAP256-VRC26.27	**16**	**9.5**	**37**	**59**	**0.05**
	CAP256-VRC26.28	**15**	**12**	**37**	**41**	**0.08**
	CAP256-VRC26.29	**15**	**13**	**37**	**46**	**0.09**
	CAP256-VRC26.30	**16**	**13**	**37**	**28**	**0.76**
	CAP256-VRC26.31	**15**	**10**	**37**	**20**	**1.66**
	CAP256-VRC26.32	**11**	**15**	**35**	**20**	**0.10**
	CAP256-VRC26.33	**9.4**	**6.5**	**35**	**22**	**0.27**

[a] Italics indicate results for antibodies published previously (21); bold font indicates the results for antibodies that are newly reported here.

(Table 1). Similarly, they varied in the rates of mutations from the inferred sequence of the UCA: 7 to 23% of the nucleotides compared with the sequence of the UCA heavy chain and 3.6 to 17% of the nucleotides compared with the sequence of the UCA lambda chain (see Table S3 in the supplemental material). All had the long CDRH3s that are characteristic of this lineage (Table 1; see Table S3 in the supplemental material): 35 or 37 amino acids, as seen previously (21), or 36 amino acids in the case of CAP256-VRC26.25. As was observed with the initial set of MAbs, the new MAbs showed no or marginal autoreactivity when tested in multiple assays (see Fig. S1 in the supplemental material).

Like the original 12 lineage members, the new CAP256-VRC26 antibodies showed a range of neutralization breadth and potency. With a 46-virus multiclade panel, their neutralization breadth varied from 2% to 63% (Table 1; see also Table S4 in the supplemental material). The member of the lineage with the broadest neutralization breadth and the most potency was CAP256-VRC26.25, which had a median IC_{50} of 0.003 μg/ml for this panel, which makes it 10-fold more potent than the most potent family members described previously (21). Two others, CAP256-VRC26.26 and CAP256-VRC26.27, also had broader neutralization than previous relatives but were not as potent as CAP256-VRC26.25. The antibodies CAP256-VRC26.19, CAP256-VRC26.22, and CAP256-VRC26.29 were similar to CAP256-VRC26.08 in neutralization breadth, neutralizing 46% of this panel (Table 1).

We also isolated antibodies that showed less neutralization breadth and potency than previously isolated family members. The sequence of the antibody with the lowest level of somatic mutation, CAP256-VRC26.24, showed only 4.2% divergence from the sequence of the heavy chain germ line and 2.5% from the

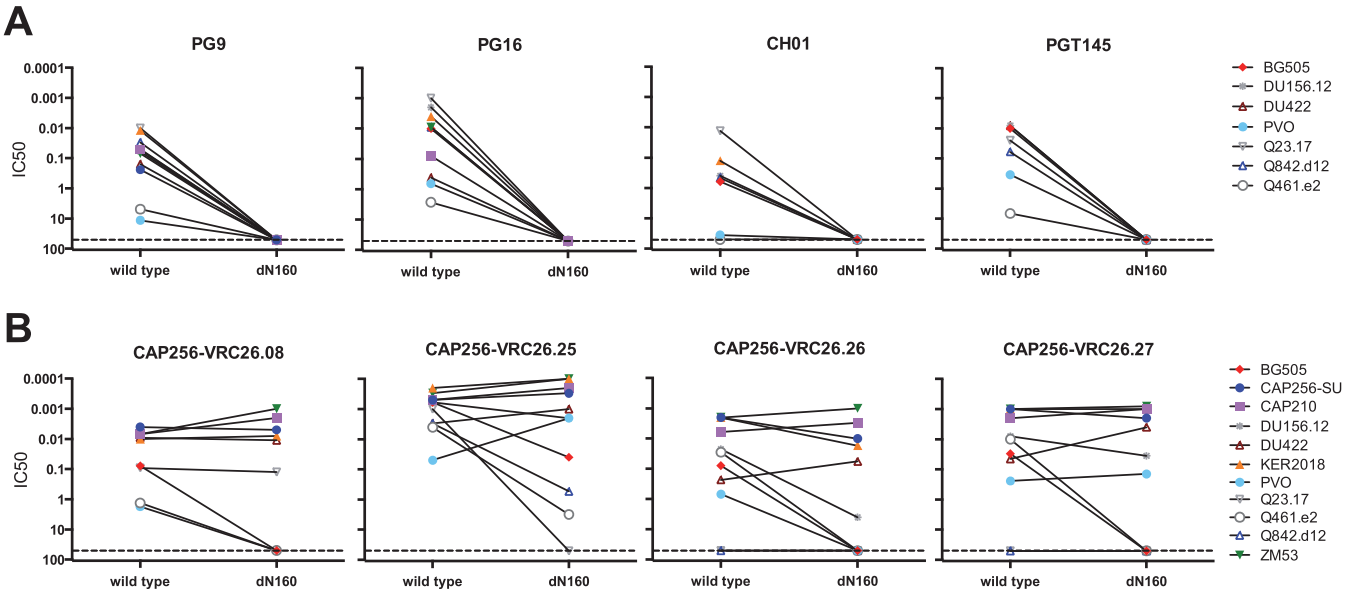

FIG 3 CAP256-VRC26 antibodies interact with N160 glycan in a potency-dependent manner. Wild-type Env pseudoviruses and mutants lacking the N160 glycan (dN160) were tested in a TZM-bl neutralization assay. Each pair of dots shows the IC_{50}s for one virus pair, with the results for the wild type being shown on the left and those for the mutant lacking the N160 glycan being shown on the right. Each graph shows data for one antibody. (A) Results for four representative PG9-like antibodies; (B) results for the four most potent CAP256-VRC26 antibodies.

sequence of the light chain. Its neutralization capacity was less broad than that of other early lineage members and it was less potent than other early lineage members, such as CAP256-VRC26.01 (Table 1). Other poor neutralizers included CAP256-VRC26.13; notably, it differed from CAP256-VRC26.12 by only 2 nucleotides or a single amino acid, even though they originated from different culture wells. An independent well yielded sequences that were 100% identical to the sequence of CAP256-VRC26.13. While these closely related lineage members were not broadly neutralizing, they did potently neutralize the autologous CAP256 superinfecting (SU) strain (see Table S4 in the supplemental material).

Like the previously identified members of the lineage (21), the new CAP256-VRC26 antibodies are highly dependent on a quaternary epitope and target V1V2. We assayed for binding to gp120 derived from HIV-1 strain CAP210, which is potently neutralized by all lineage members except CAP256-VRC26.20. None of the antibodies bound to this gp120 (see Fig. S2 in the supplemental material). CAP256-VRC26.25 was further tested on 10 additional clade C gp120s, with no binding being observed; however, it bound strongly to the BG505 SOSIP molecule, confirming the trimer preference of these antibodies. In addition, none of the 33 antibodies were able to neutralize R166A and K169E mutants in HIV-1 strain ConC (see Fig. S3A in the supplemental material), BG505.w2, or ZM53.12, and the 33 antibodies showed modest effects on ConC with mutations at amino acids 167 and 168, similar to the donor CAP256 plasma (28). Thus, the epitope recognized by the new CAP256-VRC26 antibodies is similar to that recognized by the previously described relatives.

Glycan independence of CAP256-VRC26 antibodies. The PG9-like broadly neutralizing antibodies (PG9/PG16, CH01-04, and the PGT145/PGDM1400-family antibodies) target a V1V2 epitope with quaternary epitope specificity (20, 22, 23, 59). These antibodies have been shown to require both glycan and protein contacts on Env (62, 63), with a strict dependence on the glycan at N160 (20, 22, 23, 42) and with contacts to other glycans, typically at N156 (62). We therefore investigated the glycan requirements of the CAP256-VRC26 antibodies. Removing the glycan at N156 did not abrogate neutralization; it conferred a slight decrease in potency against HIV-1 strains BG505 and ZM53 and variable effects against Q461.e2, similar to the effect that we observed with PG9 (see Fig. S3B in the supplemental material). However, removing the glycan at N160 had more dramatic effects. As expected, V1V2-directed antibodies PG9, PG16, CH01, and PGT145 were unable to neutralize glycan N160 mutants (Fig. 3A). In contrast, CAP256-VRC26 antibodies were affected in a potency-dependent manner. The N160 mutations had little effect on the susceptibility of viruses that were potently neutralized by CAP256-VRC26 antibodies but did reduce or abrogate the sensitivity of viruses that were less potently neutralized (Fig. 3B). When the data for all antibodies were combined, wild-type viruses with an IC_{50} of >0.1 μg/ml were more likely to show a neutralization reduction of at least 10-fold than the more potently neutralized viruses ($P = 0.029$, Fisher's exact test). Thus, the CAP256-VRC26 antibodies can maintain potent neutralization of viruses, despite the lack of the N160 glycan.

Phylogenetic analysis of the lineage. To deepen our understanding of the CAP256-VRC26 lineage, we placed the 12 previously cloned antibodies, together with the 21 new lineage members, within the context of total B cell transcripts. A revised algorithm (see Materials and Methods) was used to analyze 454 pyrosequencing-derived sequences from week 34 (64) and reanalyze all sequences from weeks 38 to 206 (21). Phylogenetic trees derived from maximum likelihood analysis of the transcripts of all members of the lineage, along with the 33 cloned antibody sequences, are displayed in Fig. 4. As noted previously (21), the tree for heavy chain sequences bifurcates into an upper branch and a lower branch. Sequences that map to the upper branch are plen-

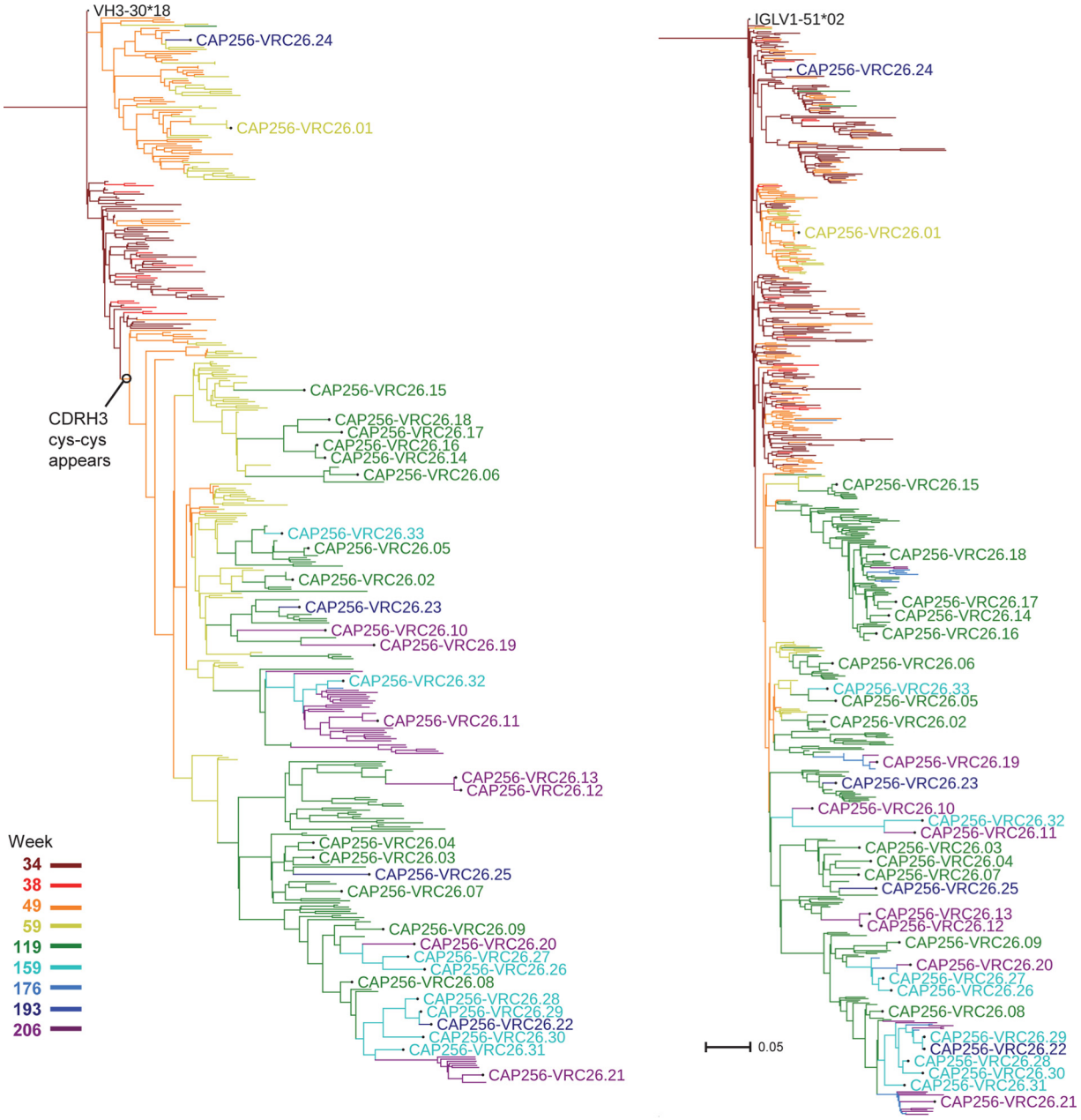

FIG 4 Development of the CAP256-VRC26 lineage. Maximum likelihood trees of heavy chain (left) and lambda chain (right) sequences. Labeled branches show heavy chains of antibodies from B cell cultures or probe sorts; unlabeled branches represent sequences from 454 pyrosequencing. The color coding indicates the time of sampling. The circle indicates the first node in which the signature Cys-Cys motif appears in the CDRH3. Scale, rate of nucleotide change (per site) between nodes.

tiful among B cell transcripts from weeks 34 to 59 but are rare among B cell transcripts obtained at week 119 or later. In contrast, the lower branch contains sequences from all time points. One notable feature of the sequences in the lower branch is a Cys-Cys which may stabilize the CDRH3 structure (21); it appears at week 49 and sequences from all subsequent times of the lower branch. Week 34 sequences do not contain Cys-Cys and appear in both the upper and lower branches of the tree.

The placement of the cloned antibodies on these trees led to several observations. The CAP256-VRC26.24 sequence is 4% mutated from the germ line sequence, clustered with week 59 sequences, and is located in the top (CAP256-VRC26.01) branch, yet it was isolated from week 193 PBMCs; we speculate that it is derived from a long-lived memory cell. CAP256-VRC26.25, the antibody with the broadest neutralization and greatest potency, has a 1-amino-acid insertion in the CDRH3 sequence compared to the UCA sequence (see Table S3 in the supplemental material) and lacks close relatives in the pyrosequencing data set, and its closest relatives are weakly neutralizing. Six of the eight antibodies that were derived from the probe sort, including the CAP256-VRC26.26 and CAP256-VRC26.27 antibodies with very broad neutralization capacities, cluster with other broad

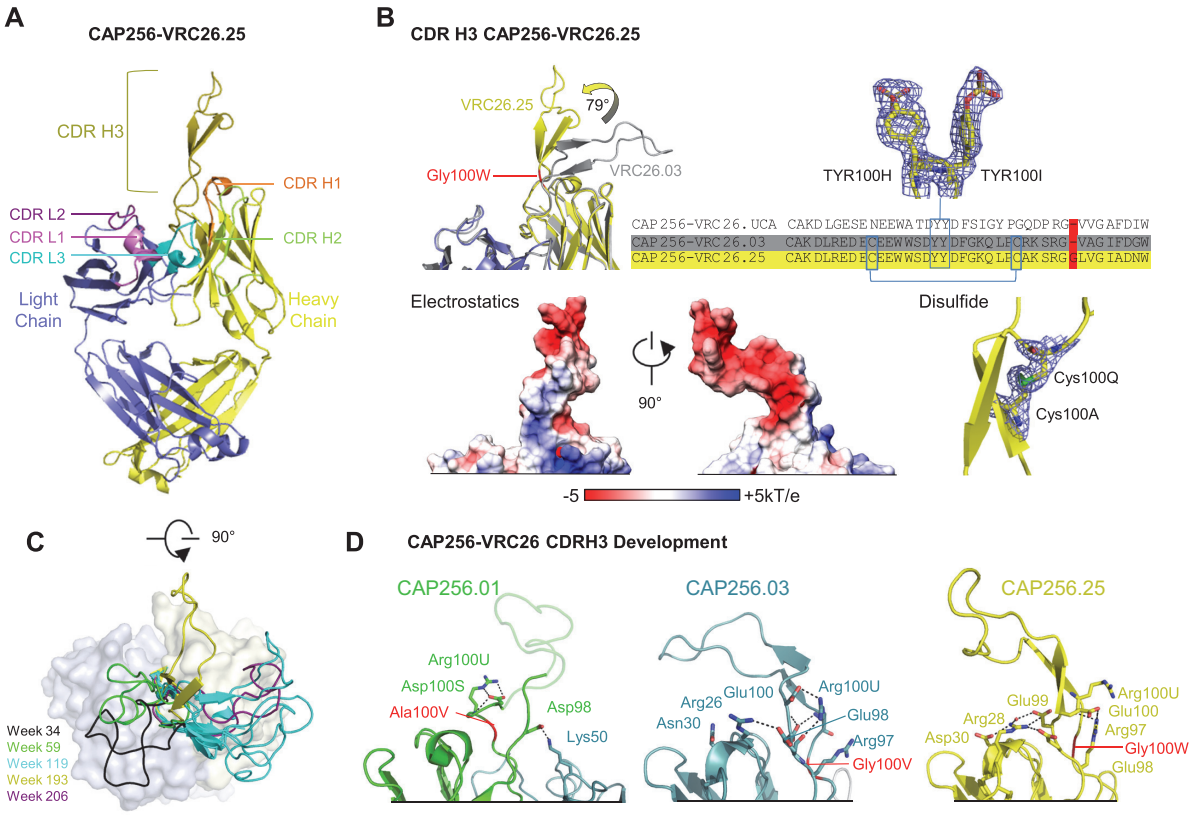

FIG 5 Structural characteristics of CAP256-VRC26.25. (A) Crystal structure of the antigen-binding fragment (Fab) of CAP256-VRC26.25 shown in ribbon diagram representation. CDRs are highlighted. (B) The CDRH3 of CAP256-VRC26.25 contains an inserted Gly and is rotated 79 degrees compared to the orientation of the other lineage members without the insertion. Gray, CAP256-VRC26.03; red, the location of the insertion in the structure and the sequence alignment. (Bottom left) The electrostatics of the highly anionic CDRH3 (charge, −7) in the same orientation in the image above. The CDRH3 contains two sulfated tyrosines and a disulfide bond (blue mesh, $2F_o$-F_c at 1 sigma). (Bottom right) Electron density of the disulfide bond acquired through affinity maturation. (C) The CDRH3s bend in different directions. All CAP256-VRC26 structures are shown, with CDRH3s projecting up from the top of the antibody. Loops are colored by the week of isolation: black, week 34, CAP256-VRC26.UCA; green, week 59, CAP256-VRC26.01; cyan, week 119, CAP256-VRC26.03, CAP256-VRC26.04, CAP256-VRC26.06, and CAP256-VRC26.07; yellow, week 193, CAP256-VRC26.25; purple, week 206, CAP256-VRC26.10. Disordered residues in the crystal structures were modeled using the Loopy program. These consist of 19, 14, 3, 11, and 10 residues for CAP256-VRC26.UCA, CAP256-VRC26.01, CAP256-VRC26.06, CAP256-VRC26.07, and CAP256-VRC26.10, respectively. All CDRH3 residues are well defined for CAP256-VRC26.03, CAP256-VRC26.04, and CAP256-VRC26.25. (D) The orientation at the base of the protruding CDRH3 loop is partially stabilized through interactions with residues in the CDRH1. Shown are interactions for CAP256-VRC26.01, CAP256-VRC26.03, and CAP256-VRC26.25. Modeled residues of CAP256-VRC26.01 are transparent.

neutralizers, CAP256-VRC26.08, CAP256-VRC26.09, and CAP256-VRC26.22; all of these bear a 2-amino-acid insertion in the CDRH3 sequence compared to the UCA sequence. However, weak neutralizers CAP256-VRC26.20, CAP256-VRC26.30, and CAP256-VRC26.31 also appear in this cluster and have this insertion. Thus, the antibodies that are the most closely genetically related do not always display the same level of neutralizing activity.

CAP256-VRC26.25 structure. To investigate the differences in neutralization potency and breadth among these antibodies, we solved the crystal structure of the CAP256-VRC26.25 antigen-binding fragment (Fab) to 2 Å. The structure was well defined, including the electron density for the entire CDRH3. Like the other lineage members, this antibody has a long CDRH3 projecting away from the body of the Fab (Fig. 5A). A disulfide bond was observed near the base of the CDRH3, as expected, and density confirming the two computationally predicted sulfated tyrosines was also visible (Fig. 5B). We compared this structure to the structures solved previously for seven other lineage members; of these, CAP256-VRC26.03 had a complete CDRH3 structure, while several others contained disordered regions of various lengths in the CDRH3 (21). Notably, the CDRH3 of CAP256-VRC26.25 bends in a considerably different direction than the others. The angle of rotation between the CDRH3s of Fabs CAP256-VRC26.03 and CAP256-VRC26.25, aligned by framework regions, is 79 degrees (Fig. 5B). When all structures are overlaid (Fig. 5C), we observe that the UCA and the early antibody CAP256-VRC26.01 bend in a similar direction, CAP256-VRC26.03, CAP256-VRC26.04, CAP256-VRC26.06, CAP256-VRC26.07, and CAP256-VRC26.10 bend in nearly the opposite direction, and CAP256-VRC26.25 bends in a direction different from the direction of all of these. The angle likely depends on the identity of amino acid at position 100V or 100W. The Gly of CAP256-VRC26.25 inserted at the base of the CDRH3 allows additional flexibility in the initial projection of the CDRH3, providing a different range of angles for the antibody to initially engage the viral spike (Fig. 5D). Thus, stabilization of the overall CDRH3 structure combined with a local flexibility at the base may contribute to the improved neutralization breadth and

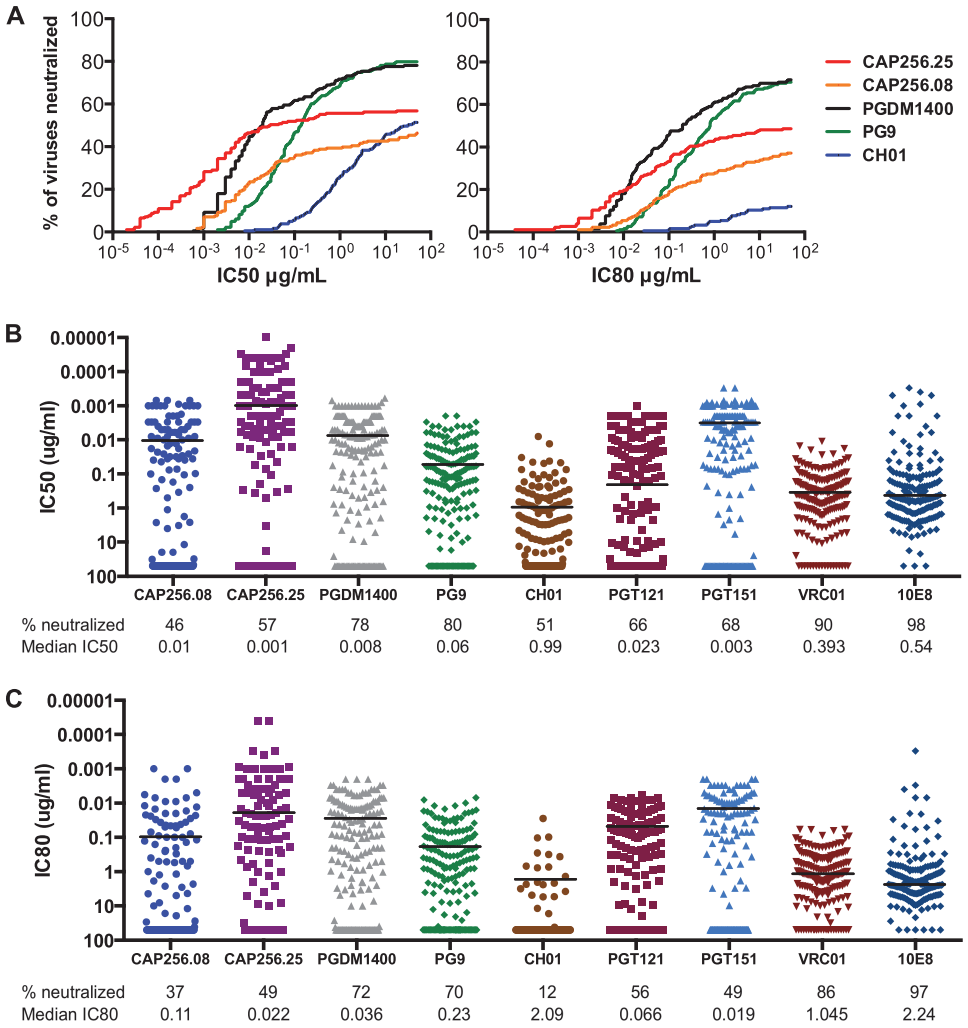

FIG 6 Neutralization breadth and potency of CAP256-VRC26.08, CAP256-VRC26.25, and selected broadly neutralizing antibodies. The neutralization of a multiclade virus panel ($n = 183$) was assessed by a TZM-bl pseudovirus assay. (A) Neutralization breadth-potency curves for V1V2-directed bNAbs. Curves show the percentage of virus neutralized at any given IC_{50} or IC_{80}. (B, C) Neutralization by bNAbs directed to diverse epitopes. Each dot shows the value for a single virus. Bars, median value of viruses that are neutralized. (B) IC_{50}s; (C) IC_{80}s.

potency of CAP256-VRC26.25 compared to those of the other lineage members.

CAP256-VRC26.25 has broad neutralization and is highly potent. CAP256-VRC26.25 is the most potent member of the lineage. On a multiclade panel of 183 Env pseudoviruses, it neutralized 57% of isolates with a median IC_{50} of 0.001 μg/ml (Fig. 6; see also Table S5 in the supplemental material), which makes it 10-fold more potent than the previously published CAP256-VRC26.08 variant. We also compared CAP256-VRC26.08 and CAP256-VRC26.25 to the V1V2-directed antibodies PGDM1400, PG9, and CH01 (Fig. 6A) and additional antibodies to other neutralization epitopes (Fig. 6B and C; see also Table S5 in the supplemental material). A remarkable characteristic of CAP256-VRC26.25 is the highly potent neutralization of some viruses. This can be seen as the leftward shift of the potency-breadth plots compared to the locations of the results for the other antibodies (Fig. 6A) and as dots close to an IC_{50} of 0.0001 μg/ml on the scatter plot (Fig. 6B).

We also examined the completeness of neutralization. Like other V1V2-directed broadly neutralizing antibodies (23, 65), the CAP256-VRC26 antibodies neutralize some viruses to a maximum of less than 90%. About 30% of sensitive viruses were neutralized with this plateau effect. This fraction is very similar to that for the V1V2-directed bNAb PGDM1400 (see Fig. S4 in the supplemental material).

To further characterize and compare the new CAP256-VRC26-lineage antibodies, we tested variants CAP256-VRC26.08, CAP256-VRC26.25, CAP256-VRC26.26, and CAP256-VRC26.27 on a multiclade panel of Env pseudoviruses (see Table S5 in the supplemental material). CAP256-VRC26.26 and CAP256-VRC26.27 have neutralization capacities nearly as broad as the neutralization capacity of CAP256-VRC26.25 at a cutoff of 50 μg/ml but less so at an IC_{50} of <0.01 μg/ml (Fig. 7A), confirming the superior potency of CAP256-VRC26.25. We also analyzed the neutralization breadth within different HIV-1 clades (Fig. 7B). Against clade C, CAP256-VRC26.25 had a neutralization breadth of 70% at the IC_{50} level (Fig. 7B; see also Fig. S5 in the supplemental material), with even greater coverage of strains from clade G

A

% Neutralized (IC50)	CAP256-VRC26.08	CAP256-VRC26.25	CAP256-VRC26.26	CAP256-VRC26.27
<50ug/ml	47	58	59	55
<10ug/ml	43	58	55	53
<1.0ug/ml	40	57	51	48
<0.1ug/ml	35	53	40	42
<0.01ug/ml	22	46	34	35

% Neutralized (IC80)	CAP256-VRC26.08	CAP256-VRC26.25	CAP256-VRC26.26	CAP256-VRC26.27
<50ug/ml	37	49	49	43
<10ug/ml	34	48	42	42
<1.0ug/ml	28	42	33	35
<0.1ug/ml	20	33	28	28
<0.01ug/ml	14	18	21	22

B

		% of viruses neutralized (IC50<50)			
Clade	N	CAP256-VRC26.08	CAP256-VRC26.25	CAP256-VRC26.26	CAP256-VRC26.27
A	26	46	69	58	58
AE	21	43	48	57	57
AG	16	56	81	69	69
B	40	3	15	13	10
BC	10	70	100	80	80
C	57	67	70	72	67
D	8	50	63	75	63
G	7	57	71	71	71
other	13	69	69	69	62
All	198	47	58	59	55
non-B	158	58	70	68	65

		% of viruses neutralized (IC80<50)			
Clade	N	CAP256-VRC26.08	CAP256-VRC26.25	CAP256-VRC26.26	CAP256-VRC26.27
A	26	27	54	38	35
AE	21	33	48	52	48
AG	16	50	69	63	56
B	40	0	10	8	3
BC	10	60	80	60	60
C	57	53	60	63	60
D	8	38	63	50	50
G	7	57	71	71	57
other	13	62	62	46	46
All	198	37	49	49	43
non-B	158	46	60	56	52

other: AC, ACD, AD, CD

FIG 7 Neutralization breadth, potency, and clade dependency of CAP256-VRC26 antibodies. The neutralization of large virus panels was assessed by a TZM-bl pseudovirus assay. (Left) IC_{50}s; (right) IC_{80}s. (A) Values indicate the percentage of viruses ($n = 198$) neutralized at the given cutoff; (B) values indicate the percentage of viruses neutralized within each virus clade.

and circulating recombinant forms AG and BC. While CAP256-VRC26.25 neutralized 70% of non-clade B strains overall, it neutralized only 15% of clade B strains. To understand the basis of this preference, we performed an amino acid frequency analysis (53) for positions 154 to 184 in V2. Specifically, based on sequence alignments, we searched for amino acids that were preferentially found among CAP256-VRC26.25-resistant strains versus CAP256-VRC26.25-sensitive strains for each residue position in V2 (Fig. 8A). Amino acids that were associated with resistance were found in at least one position among positions 166, 167, and 169 in 59% of resistant strains. These amino acids were observed in 71% of clade B strains and in 80% of resistant clade B strains. Conversely, the amino acid K or R at position 169 occurred in 86% of sensitive strains but in only 5% of clade B strains, with similar proportions occurring for D or E at position 164 (Fig. 8B). The occurrence of resistance-associated amino acids at one or more of these positions was statistically significant ($P < 0.001$ for each comparison, Fisher's exact test), as was the occurrence of the sensitivity-associated amino acids at positions 164 and 169. Thus, the characteristics of clade B sequences at V2 positions 164, 166, 167, and 169 may explain much of the resistance found in clade B strains.

DISCUSSION

The data in this study provide a more comprehensive picture of the CAP256-VRC26 bNAb lineage. Using modified PCR primers, B cell culture, and trimeric Env-based probes, we isolated 21 new members of the CAP256-VRC26 family. Several of these new antibodies showed an increased neutralization breadth and potency compared to those of previously published antibodies of this lineage, particularly against HIV-1 clade C strains and other subtypes prevalent in sub-Saharan Africa. CAP256-VRC26.25 in particular showed exceptional potency, with a median IC_{50} against neutralized viruses of 0.001 μg/ml.

We isolated new clonal relatives of the CAP256-VRC26 lineage by two methods: B cell culture and antigen-specific B cell sorting. The differential BG505 SOSIP and BG505 SOSIP.K169E protein sorting approach proved to be a highly efficient and specific method for isolating new members of the CAP256-VRC26 lineage. Here, 11/14 sorted cells yielded CAP256-VRC26-lineage members, and two of the three most broadly neutralizing lineage members were isolated from the probe sort. The availability of nearly native trimers has potential for use in sorting for V1V2-directed and other quaternary epitope-specific antibodies in other donors (59), while the K169E mutant described here may have utility for additional donors with serum neutralization dependence on this V2 residue. However, this method has some limitations. Not all Env epitopes are displayed on the BG505 SOSIP molecule: the MPER region of gp41 is not contained in this construct, and some antibodies may not recognize the BG505 sequence. With regard to differential sorting with a knockout mutant, not all donors have neutralization activity that can be matched to that of a wild-type probe–mutant probe pair. Thus, the advantage of B cell culture is that it does not require a probe or, indeed, any *a priori* knowledge of the antibody specificity. Additionally, since the wells are screened by neutralization, there may be selection for the detection of highly potent antibodies. However, B cell culture is more labor-intensive and time-consuming than single-cell sorting and is most successful when the donor has high plasma neutralization titers (N. A. Doria-Rose and N. Longo, unpublished observations). In addition, culture conditions can induce *in vitro* class switching, which complicates the recovery

A

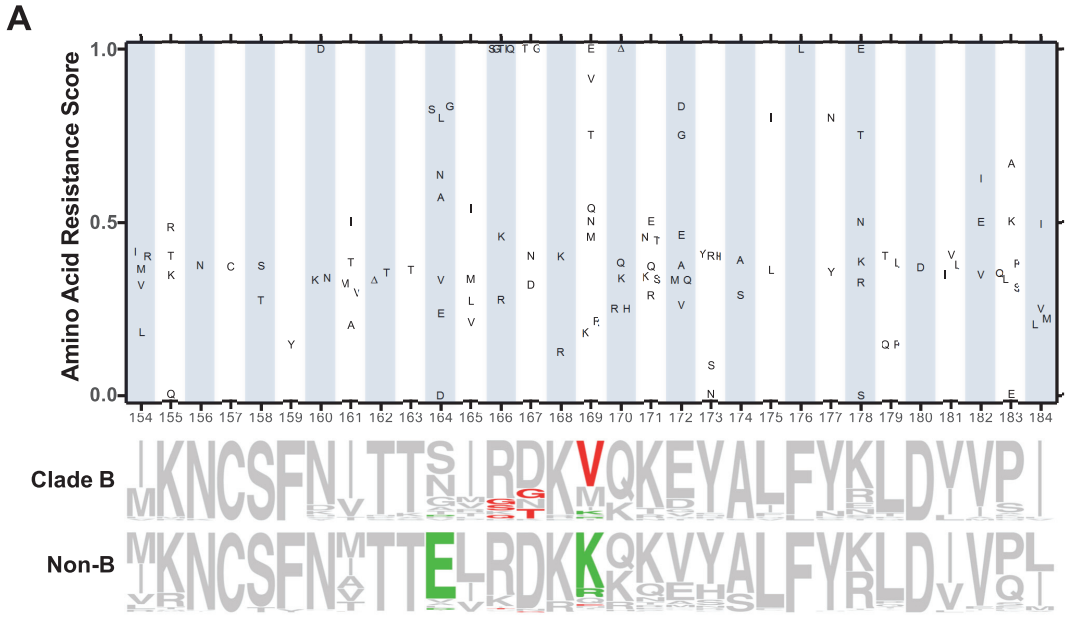

B

Association	Position	Amino Acid	% of sequences with the indicated amino acid			
			Sensitive	Resistant	Non-Clade B	Clade B
Sensitivity	164	D or E	84%	42%	85%	3%
	169	R or K	86%	33%	81%	5%
Resistance	166	G,I,Q,S, or T	0%	23%	6%	20%
	167	T or G	0%	18%	2%	25%
	169	E or V	2%	34%	3%	55%
	one or more of the above		2%	59%	10%	73%

FIG 8 CAP256-VRC26.25 resistance analysis of amino acids in Env V2. (A) (Top) Amino acid frequency analysis. A total of 198 sequences were analyzed (see Fig. S6 in the supplemental material). The resistance score for each possible amino acid at a given residue position was defined as the ratio of its number of occurrences in sequences from CAP256-VRC26.25-resistant viruses to its overall number of occurrences. A higher score indicates that the amino acid was preferentially found among sequences from resistant viruses, with a score of 1 indicating that the amino was found only among sequences from resistant viruses. Amino acids that occurred at least 3 times at the given position are shown. (Bottom) Logo plot showing the frequency of all amino acids at each position for clade B ($n = 40$) and non-clade B ($n = 158$) sequences. Red, amino acids associated with resistance; green, amino acids associated with sensitivity. (B) Frequency of amino acids at positions associated with resistance or sensitivity. Values indicate the percentage of sequences in a given category that bear the indicated amino acids. For example, 84% of Env sequences from sensitive strains have D or E at position 164. A total of 125 sensitive strains and 73 resistant strains were analyzed. *P* was <0.001 for each comparison (Fisher's exact test with the Bonferroni correction).

of sequences by PCR, though this can be overcome by using IgA constant region primers. Of note, the most potent member of the lineage (CAP256-VRC26.25) was isolated from a B cell culture, attesting to the advantages of high-throughput functional screening.

Phylogenetic analysis of the complete CAP256-VRC26 lineage shows two main branches. The first branch, which included CAP256-VRC26.01 and CAP256-VRC26.24, may be an evolutionary dead end, in that members of the branch could not be detected in the B cell transcripts from time points after week 119. We recently showed that the antibodies in this branch were unable to tolerate viral escape mutations and were no longer selected for (64). The Cys-Cys disulfide bond in CDRH3 emerged in the second branch, and that sublineage continued to evolve, with sequences being observed at all time points. Within this sublineage, however, antibodies with broad or narrow heterologous neutralization are intermingled. This suggests that individual amino acid changes, rather than overall sequence relatedness, have greater effects on the neutralization capacity. Similarly, the levels of mutation compared with the sequence of the germ line V gene or that of the UCA did not correlate with neutralization. A similar pattern has been noted for other bNAb lineages (22, 59, 66). These observations suggest that somatic variant antibodies with a variety of antiviral capacities frequently evolve side-by-side during chronic HIV infection. The concurrent diversification of the viral quasispecies may drive this evolution: while some antibody mutations may improve the binding to specific autologous viral variants encountered in the germinal center, they may not be the same mutations that improve the neutralization breadth against heterologous viruses.

The CAP256-VRC26 antibodies share many characteristics with the three other published lineages of V1V2 directed broadly neutralizing antibodies: the PG9, PGT145, and CH01 lineages (20, 22, 23, 59). These antibodies have long, anionic CDRH3s, exhibit incomplete neutralization of some viruses (65), and share epitope requirements: they are highly quaternary epitope specific and pre-

fer positive charges in strand C of V2 (53), and their activity is knocked out by a K169E mutation. However, in contrast to the three other lineages, which show a strong dependence on the N160 glycan (Fig. 3) (42), the CAP256-VRC26 antibodies showed variable and limited dependence on this glycan. The more potent that the antibody-mediated neutralization was, the less dependent it was on the presence of the N160 glycan. We speculate that potent neutralization is mediated mainly by protein-protein contacts but that more weakly recognized strains are bound via contacts with both protein and glycan. It is also possible that alternative glycans are bound when the N160 glycan is missing. Future structural studies may provide a better understanding of the mechanism. Notably, a mutant form of PG9 with increased potency was shown to neutralize some viruses lacking the N160 glycan (67); this observation is consistent with the notion that the very high potency of CAP256-VRC26.25 may relate to the lack of N160 glycan dependency.

CAP256-VRC26.25 neutralized 15% of clade B HIV-1 strains and 70% of non-clade B HIV-1 strains. Amino acids associated with sensitivity or resistance were noted at positions 164, 166, 167, and 169. The residues associated with sensitivity—D or E at position 164 and R or K at position 169—were rare in clade B; conversely, resistance-associated amino acids were more common in clade B strains than non-clade B strains. Of note, several of these preferences mirror the neutralization activity of the donor's plasma (28); furthermore, escape mutations that arose in the CAP256 donor virus near the time point of CAP256-VRC26.25 isolation include S at position 166 and E at position 169 (21, 64), both of which were associated with resistance in this virus panel.

In summary, we isolated 21 new members of the CAP256-VRC26 lineage, including 3 variants that have a broader neutralization capacity than the previously isolated family members. The best variant, CAP256-VRC26.25, was 10-fold more potent than the previously published members of this lineage, and its overall potency (IC_{50} = 0.001 μg/ml) was comparable to or better than that of existing bNAbs. In addition, the neutralization capacity of CAP256-VRC26.25 was quite broad, neutralizing ~60% of all viruses and ~ 70% of non-clade B viruses, including clade C viruses. The mechanism of its outstanding potency may relate to the reduced dependence on N160 glycan, the unique CDRH3 conformation, or other structural features that have yet to be elucidated. The high potency of this antibody may make it an attractive candidate for clinical development for prevention of infection or as part of antiretroviral regimens to treat HIV-1 infection.

ACKNOWLEDGMENTS

We thank the participants in the CAPRISA 002 study for their commitment. For technical assistance and advice, we thank the CAPRISA 002 clinical team, Natasha Samsunder, Shannie Heeralall, Ellen Turk, Chien-Li Lin, and Robert Banks. We thank Nancy S. Longo, Johannes Scheid, and Xueling Wu for advice on the development of PCR protocols and Brenda Hartman and Andrea Shiakolas for assistance with manuscript preparation. We thank J. Baalwa, D. Ellenberger, F. Gao, B. Hahn, K. Hong, J. Kim, F. McCutchan, D. Montefiori, L. Morris, J. Overbaugh, E. Sanders-Buell, G. Shaw, R. Swanstrom, M. Thomson, S. Tovanabutra, C. Williamson, and L. Zhang for contributing the HIV-1 envelope plasmids used in our neutralization panel.

FUNDING INFORMATION

National Institutes of Health provided funding to Penny L. Moore, Lynn Morris, Peter D. Kwong, and John R. Mascola under grant number AI116086-01. South African Medical Research Council provided funding to Penny L. Moore under grant number D1407250-01. Wellcome Trust provided funding to Penny L. Moore under grant number 089933/Z/09/Z.

CAPRISA is funded by the South African HIV/AIDS Research and Innovation Platform of the South African Department of Science and Technology and was initially supported by National Institute of Allergy and Infectious Diseases, National Institutes of Health, U.S. Department of Health and Human Services, grant U19 AI51794 (to Salim Abdool-Karim). The Columbia University-Southern African Fogarty AIDS International Training and Research Program, through the Fogarty International Center, National Institutes of Health, provided funding to Jinal N. Bhiman, Penny L. Moore, and Lynn Morris under grant number 5 D43 TW000231. Jinal N. Bhiman received a University of the Witwatersrand Postgraduate Merit Award as well as bursaries from the Poliomyelitis Research Foundation and the National Research Foundation of South Africa. Funding was provided by the intramural research programs of the Vaccine Research Center, Division of Intramural Research, National Institute of Allergy and Infectious Diseases, National Institutes of Health, USA. Use of sector 22 (Southeast Region Collaborative Access Team) at the Advanced Photon Source was supported by the US Department of Energy, Basic Energy Sciences, Office of Science, under contract number W-31-109-Eng-38. The funders had no role in study design, data collection and interpretation, or the decision to submit the work for publication.

REFERENCES

1. **Doria-Rose NA, Klein RM, Daniels MG, O'Dell S, Nason M, Lapedes A, Bhattacharya T, Migueles SA, Wyatt RT, Korber BT, Mascola JR, Connors M.** 2010. Breadth of human immunodeficiency virus-specific neutralizing activity in sera: clustering analysis and association with clinical variables. J Virol **84:**1631–1636. http://dx.doi.org/10.1128/JVI.01482-09.
2. **Hraber P, Seaman MS, Bailer RT, Mascola JR, Montefiori DC, Korber BT.** 2014. Prevalence of broadly neutralizing antibody responses during chronic HIV-1 infection. AIDS **28:**163–169. http://dx.doi.org/10.1097/QAD.0000000000000106.
3. **Simek MD, Rida W, Priddy FH, Pung P, Carrow E, Laufer DS, Lehrman JK, Boaz M, Tarragona-Fiol T, Miiro G, Birungi J, Pozniak A, McPhee DA, Manigart O, Karita E, Inwoley A, Jaoko W, Dehovitz J, Bekker LG, Pitisuttithum P, Paris R, Walker LM, Poignard P, Wrin T, Fast PE, Burton DR, Koff WC.** 2009. Human immunodeficiency virus type 1 elite neutralizers: individuals with broad and potent neutralizing activity identified by using a high-throughput neutralization assay together with an analytical selection algorithm. J Virol **83:**7337–7348. http://dx.doi.org/10.1128/JVI.00110-09.
4. **Sather DN, Armann J, Ching LK, Mavrantoni A, Sellhorn G, Caldwell Z, Yu X, Wood B, Self S, Kalams S, Stamatatos L.** 2009. Factors associated with the development of cross-reactive neutralizing antibodies during human immunodeficiency virus type 1 infection. J Virol **83:**757–769. http://dx.doi.org/10.1128/JVI.02036-08.
5. **Mascola JR, Haynes BF.** 2013. HIV-1 neutralizing antibodies: understanding nature's pathways. Immunol Rev **254:**225–244. http://dx.doi.org/10.1111/imr.12075.
6. **Excler JL, Robb ML, Kim JH.** 2015. Prospects for a globally effective HIV-1 vaccine. Vaccine http://dx.doi.org/10.1016/j.vaccine.2015.03.059.
7. **Overbaugh J, Morris L.** 2012. The antibody response against HIV-1. Cold Spring Harb Perspect Med **2:**a007039. http://dx.doi.org/10.1101/cshperspect.a007039.
8. **Klein F, Mouquet H, Dosenovic P, Scheid JF, Scharf L, Nussenzweig MC.** 2013. Antibodies in HIV-1 vaccine development and therapy. Science **341:**1199–1204. http://dx.doi.org/10.1126/science.1241144.
9. **Doria-Rose NA, Joyce MG.** 2015. Strategies to guide the antibody affinity maturation process. Curr Opin Virol **11:**137–147. http://dx.doi.org/10.1016/j.coviro.2015.04.002.
10. **Haynes BF, Kelsoe G, Harrison SC, Kepler TB.** 2012. B-cell-lineage

immunogen design in vaccine development with HIV-1 as a case study. Nat Biotechnol **30:**423–433. http://dx.doi.org/10.1038/nbt.2197.

11. **Julien JP, Cupo A, Sok D, Stanfield RL, Lyumkis D, Deller MC, Klasse PJ, Burton DR, Sanders RW, Moore JP, Ward AB, Wilson IA.** 2013. Crystal structure of a soluble cleaved HIV-1 envelope trimer. Science **342:** 1477–1483. http://dx.doi.org/10.1126/science.1245625.
12. **Pancera M, Zhou T, Druz A, Georgiev IS, Soto C, Gorman J, Huang J, Acharya P, Chuang GY, Ofek G, Stewart-Jones GB, Stuckey J, Bailer RT, Joyce MG, Louder MK, Tumba N, Yang Y, Zhang B, Cohen MS, Haynes BF, Mascola JR, Morris L, Munro JB, Blanchard SC, Mothes W, Connors M, Kwong PD.** 2014. Structure and immune recognition of trimeric pre-fusion HIV-1 Env. Nature **514:**455–461. http://dx.doi.org/10.1038/nature13808.
13. **Lyumkis D, Julien JP, de Val N, Cupo A, Potter CS, Klasse PJ, Burton DR, Sanders RW, Moore JP, Carragher B, Wilson IA, Ward AB.** 2013. Cryo-EM structure of a fully glycosylated soluble cleaved HIV-1 envelope trimer. Science **342:**1484–1490. http://dx.doi.org/10.1126/science.1245627.
14. **Kwong PD, Mascola JR.** 2012. Human antibodies that neutralize HIV-1: identification, structures, and B cell ontogenies. Immunity **37:**412–425. http://dx.doi.org/10.1016/j.immuni.2012.08.012.
15. **Wibmer CK, Moore PL, Morris L.** 2015. HIV broadly neutralizing antibody targets. Curr Opin HIV AIDS **10:**135–143. http://dx.doi.org/10.1097/COH.0000000000000153.
16. **Burton DR, Mascola JR.** 2015. Antibody responses to envelope glycoproteins in HIV-1 infection. Nat Immunol **16:**571–576. http://dx.doi.org/10.1038/ni.3158.
17. **Kwong PD, Mascola JR, Nabel GJ.** 2013. Broadly neutralizing antibodies and the search for an HIV-1 vaccine: the end of the beginning. Nat Rev Immunol **13:**693–701. http://dx.doi.org/10.1038/nri3516.
18. **Walker LM, Simek MD, Priddy F, Gach JS, Wagner D, Zwick MB, Phogat SK, Poignard P, Burton DR.** 2010. A limited number of antibody specificities mediate broad and potent serum neutralization in selected HIV-1 infected individuals. PLoS Pathog **6:**e1001028. http://dx.doi.org/10.1371/journal.ppat.1001028.
19. **Georgiev IS, Doria-Rose NA, Zhou T, Kwon YD, Staupe RP, Moquin S, Chuang GY, Louder MK, Schmidt SD, Altae-Tran HR, Bailer RT, McKee K, Nason M, O'Dell S, Ofek G, Pancera M, Srivatsan S, Shapiro L, Connors M, Migueles SA, Morris L, Nishimura Y, Martin MA, Mascola JR, Kwong PD.** 2013. Delineating antibody recognition in polyclonal sera from patterns of HIV-1 isolate neutralization. Science **340:** 751–756. http://dx.doi.org/10.1126/science.1233989.
20. **Bonsignori M, Hwang KK, Chen X, Tsao CY, Morris L, Gray E, Marshall DJ, Crump JA, Kapiga SH, Sam NE, Sinangil F, Pancera M, Yongping Y, Zhang B, Zhu J, Kwong PD, O'Dell S, Mascola JR, Wu L, Nabel GJ, Phogat S, Seaman MS, Whitesides JF, Moody MA, Kelsoe G, Yang X, Sodroski J, Shaw GM, Montefiori DC, Kepler TB, Tomaras GD, Alam SM, Liao HX, Haynes BF.** 2011. Analysis of a clonal lineage of HIV-1 envelope V2/V3 conformational epitope-specific broadly neutralizing antibodies and their inferred unmutated common ancestors. J Virol **85:**9998–10009. http://dx.doi.org/10.1128/JVI.05045-11.
21. **Doria-Rose NA, Schramm CA, Gorman J, Moore PL, Bhiman JN, DeKosky BJ, Ernandes MJ, Georgiev IS, Kim HJ, Pancera M, Staupe RP, Altae-Tran HR, Bailer RT, Crooks ET, Cupo A, Druz A, Garrett NJ, Hoi KH, Kong R, Louder MK, Longo NS, McKee K, Nonyane M, O'Dell S, Roark RS, Rudicell RS, Schmidt SD, Sheward DJ, Soto C, Wibmer CK, Yang Y, Zhang Z, Mullikin JC, Binley JM, Sanders RW, Wilson IA, Moore JP, Ward AB, Georgiou G, Williamson C, Abdool Karim SS, Morris L, Kwong PD, Shapiro L, Mascola JR.** 2014. Developmental pathway for potent V1V2-directed HIV-neutralizing antibodies. Nature **509:**55–62. http://dx.doi.org/10.1038/nature13036.
22. **Walker LM, Huber M, Doores KJ, Falkowska E, Pejchal R, Julien JP, Wang SK, Ramos A, Chan-Hui PY, Moyle M, Mitcham JL, Hammond PW, Olsen OA, Phung P, Fling S, Wong CH, Phogat S, Wrin T, Simek MD, Koff WC, Wilson IA, Burton DR, Poignard P.** 2011. Broad neutralization coverage of HIV by multiple highly potent antibodies. Nature **477:**466–470. http://dx.doi.org/10.1038/nature10373.
23. **Walker LM, Phogat SK, Chan-Hui PY, Wagner D, Phung P, Goss JL, Wrin T, Simek MD, Fling S, Mitcham JL, Lehrman JK, Priddy FH, Olsen OA, Frey SM, Hammond PW, Kaminsky S, Zamb T, Moyle M, Koff WC, Poignard P, Burton DR.** 2009. Broad and potent neutralizing antibodies from an African donor reveal a new HIV-1 vaccine target. Science **326:**285–289. http://dx.doi.org/10.1126/science.1178746.
24. **Julien JP, Lee JH, Cupo A, Murin CD, Derking R, Hoffenberg S, Caulfield MJ, King CR, Marozsan AJ, Klasse PJ, Sanders RW, Moore JP, Wilson IA, Ward AB.** 2013. Asymmetric recognition of the HIV-1 trimer by broadly neutralizing antibody PG9. Proc Natl Acad Sci U S A **110:**4351–4356. http://dx.doi.org/10.1073/pnas.1217537110.
25. **Huang J, Kang BH, Pancera M, Lee JH, Tong T, Feng Y, Imamichi H, Georgiev IS, Chuang GY, Druz A, Doria-Rose NA, Laub L, Sliepen K, van Gils MJ, de la Pena AT, Derking R, Klasse PJ, Migueles SA, Bailer RT, Alam M, Pugach P, Haynes BF, Wyatt RT, Sanders RW, Binley JM, Ward AB, Mascola JR, Kwong PD, Connors M.** 2014. Broad and potent HIV-1 neutralization by a human antibody that binds the gp41-gp120 interface. Nature **515:**138–142. http://dx.doi.org/10.1038/nature13601.
26. **Pinter A, Honnen WJ, He Y, Gorny MK, Zolla-Pazner S, Kayman SC.** 2004. The V1/V2 domain of gp120 is a global regulator of the sensitivity of primary human immunodeficiency virus type 1 isolates to neutralization by antibodies commonly induced upon infection. J Virol **78:**5205–5215. http://dx.doi.org/10.1128/JVI.78.10.5205-5215.2004.
27. **Doores KJ, Burton DR.** 2010. Variable loop glycan dependency of the broad and potent HIV-1-neutralizing antibodies PG9 and PG16. J Virol **84:**10510–10521. http://dx.doi.org/10.1128/JVI.00552-10.
28. **Moore PL, Gray ES, Sheward D, Madiga M, Ranchobe N, Lai Z, Honnen WJ, Nonyane M, Tumba N, Hermanus T, Sibeko S, Mlisana K, Abdool Karim SS, Williamson C, Pinter A, Morris L.** 2011. Potent and broad neutralization of HIV-1 subtype C by plasma antibodies targeting a quaternary epitope including residues in the V2 loop. J Virol **85:**3128–3141. http://dx.doi.org/10.1128/JVI.02658-10.
29. **Moore PL, Sheward D, Nonyane M, Ranchobe N, Hermanus T, Gray ES, Abdool Karim SS, Williamson C, Morris L.** 2013. Multiple pathways of escape from HIV broadly cross-neutralizing V2-dependent antibodies. J Virol **87:**4882–4894. http://dx.doi.org/10.1128/JVI.03424-12.
30. **van Loggerenberg F, Mlisana K, Williamson C, Auld SC, Morris L, Gray CM, Abdool Karim Q, Grobler A, Barnabas N, Iriogbe I, Abdool Karim SS, CAPRISA 002 Acute Infection Study Team.** 2008. Establishing a cohort at high risk of HIV infection in South Africa: challenges and experiences of the CAPRISA 002 acute infection study. PLoS One **3:**e1954. http://dx.doi.org/10.1371/journal.pone.0001954.
31. **Gray ES, Madiga MC, Hermanus T, Moore PL, Wibmer CK, Tumba NL, Werner L, Mlisana K, Sibeko S, Williamson C, Abdool Karim SS, Morris L.** 2011. The neutralization breadth of HIV-1 develops incrementally over four years and is associated with $CD4^+$ T cell decline and high viral load during acute infection. J Virol **85:**4828–4840. http://dx.doi.org/10.1128/JVI.00198-11.
32. **Huang J, Doria-Rose NA, Longo NS, Laub L, Lin CL, Turk E, Kang BH, Migueles SA, Bailer RT, Mascola JR, Connors M.** 2013. Isolation of human monoclonal antibodies from peripheral blood B cells. Nat Protoc **8:**1907–1915. http://dx.doi.org/10.1038/nprot.2013.117.
33. **Huang J, Ofek G, Laub L, Louder MK, Doria-Rose NA, Longo NS, Imamichi H, Bailer RT, Chakrabarti B, Sharma SK, Alam SM, Wang T, Yang Y, Zhang B, Migueles SA, Wyatt R, Haynes BF, Kwong PD, Mascola JR, Connors M.** 2012. Broad and potent neutralization of HIV-1 by a gp41-specific human antibody. Nature **491:**406–412. http://dx.doi.org/10.1038/nature11544.
34. **Doria-Rose N, Bailer R, Louder M, Lin C-L, Turk E, Laub L, Longo N, Connors M, Mascola J.** 13 September 2013. High throughput HIV-1 microneutralization assay. Protocol Exchange. http://dx.doi.org/10.1038/protex.2013.069.
35. **Sanders RW, Derking R, Cupo A, Julien JP, Yasmeen A, de Val N, Kim HJ, Blattner C, de la Pena AT, Korzun J, Golabek M, de Los Reyes K, Ketas TJ, van Gils MJ, King CR, Wilson IA, Ward AB, Klasse PJ, Moore JP.** 2013. A next-generation cleaved, soluble HIV-1 Env trimer, BG505 SOSIP.664 gp140, expresses multiple epitopes for broadly neutralizing but not non-neutralizing antibodies. PLoS Pathog **9:**e1003618. http://dx.doi.org/10.1371/journal.ppat.1003618.
36. **Wu X, Yang ZY, Li Y, Hogerkorp CM, Schief WR, Seaman MS, Zhou T, Schmidt SD, Wu L, Xu L, Longo NS, McKee K, O'Dell S, Louder MK, Wycuff DL, Feng Y, Nason M, Doria-Rose N, Connors M, Kwong PD, Roederer M, Wyatt RT, Nabel GJ, Mascola JR.** 2010. Rational design of envelope identifies broadly neutralizing human monoclonal antibodies to HIV-1. Science **329:**856–861. http://dx.doi.org/10.1126/science.1187659.
37. **Tiller T, Meffre E, Yurasov S, Tsuiji M, Nussenzweig MC, Wardemann H.** 2008. Efficient generation of monoclonal antibodies from

single human B cells by single cell RT-PCR and expression vector cloning. J Immunol Methods **329:**112–124. http://dx.doi.org/10.1016/j.jim.2007.09.017.

38. **Scheid JF, Mouquet H, Ueberheide B, Diskin R, Klein F, Oliveira TY, Pietzsch J, Fenyo D, Abadir A, Velinzon K, Hurley A, Myung S, Boulad F, Poignard P, Burton DR, Pereyra F, Ho DD, Walker BD, Seaman MS, Bjorkman PJ, Chait BT, Nussenzweig MC.** 2011. Sequence and structural convergence of broad and potent HIV antibodies that mimic CD4 binding. Science **333:**1633–1637. http://dx.doi.org/10.1126/science.1207227.
39. **Liao HX, Levesque MC, Nagel A, Dixon A, Zhang R, Walter E, Parks R, Whitesides J, Marshall DJ, Hwang KK, Yang Y, Chen X, Gao F, Munshaw S, Kepler TB, Denny T, Moody MA, Haynes BF.** 2009. High-throughput isolation of immunoglobulin genes from single human B cells and expression as monoclonal antibodies. J Virol Methods **158:**171–179. http://dx.doi.org/10.1016/j.jviromet.2009.02.014.
40. **Shu Y, Winfrey S, Yang ZY, Xu L, Rao SS, Srivastava I, Barnett SW, Nabel GJ, Mascola JR.** 2007. Efficient protein boosting after plasmid DNA or recombinant adenovirus immunization with HIV-1 vaccine constructs. Vaccine **25:**1398–1408. http://dx.doi.org/10.1016/j.vaccine.2006.10.046.
41. **Montefiori DC.** 2009. Measuring HIV neutralization in a luciferase reporter gene assay. Methods Mol Biol **485:**395–405. http://dx.doi.org/10.1007/978-1-59745-170-3_26.
42. **Wu X, Changela A, O'Dell S, Schmidt SD, Pancera M, Yang Y, Zhang B, Gorny MK, Phogat S, Robinson JE, Stamatatos L, Zolla-Pazner S, Kwong PD, Mascola JR.** 2011. Immunotypes of a quaternary site of HIV-1 vulnerability and their recognition by antibodies. J Virol **85:**4578–4585. http://dx.doi.org/10.1128/JVI.02585-10.
43. **Haynes BF, Fleming J, St Clair EW, Katinger H, Stiegler G, Kunert R, Robinson J, Scearce RM, Plonk K, Staats HF, Ortel TL, Liao HX, Alam SM.** 2005. Cardiolipin polyspecific autoreactivity in two broadly neutralizing HIV-1 antibodies. Science **308:**1906–1908. http://dx.doi.org/10.1126/science.1111781.
44. **Wu X, Zhang Z, Schramm CA, Joyce MG, Do Kwon Y, Zhou T, Sheng Z, Zhang B, O'Dell S, McKee K, Georgiev IS, Chuang GY, Longo NS, Lynch RM, Saunders KO, Soto C, Srivatsan S, Yang Y, Bailer RT, Louder MK, NISC Comparative Sequencing Program, Mullikin JC, Connors M, Kwong PD, Mascola JR, Shapiro L.** 2015. Maturation and diversity of the VRC01-antibody lineage over 15 years of chronic HIV-1 infection. Cell **161:**470–485. http://dx.doi.org/10.1016/j.cell.2015.03.004.
45. **Li W, Jaroszewski L, Godzik A.** 2001. Clustering of highly homologous sequences to reduce the size of large protein databases. Bioinformatics **17:**282–283. http://dx.doi.org/10.1093/bioinformatics/17.3.282.
46. **Ashkenazy H, Penn O, Doron-Faigenboim A, Cohen O, Cannarozzi G, Zomer O, Pupko T.** 2012. FastML: a web server for probabilistic reconstruction of ancestral sequences. Nucleic Acids Res **40:**W580–W584. http://dx.doi.org/10.1093/nar/gks498.
47. **Felsenstein J.** 2005. PHYLIP (phylogeny inference package) version 3.6. http://cmgm.stanford.edu/phylip/dnaml.html.
48. **Otwinowski Z, Minor W.** 1997. Processing of X-ray diffraction data collected in oscillation mode. Methods Enzymol **276:**307–326. http://dx.doi.org/10.1016/S0076-6879(97)76066-X.
49. **Emsley P, Cowtan K.** 2004. Coot: model-building tools for molecular graphics. Acta Crystallogr D Biol Crystallogr **60:**2126–2132. http://dx.doi.org/10.1107/S0907444904019158.
50. **Adams PD, Gopal K, Grosse-Kunstleve RW, Hung LW, Ioerger TR, McCoy AJ, Moriarty NW, Pai RK, Read RJ, Romo TD, Sacchettini JC, Sauter NK, Storoni LC, Terwilliger TC.** 2004. Recent developments in the PHENIX software for automated crystallographic structure determination. J Synchrotron Radiat **11:**53–55. http://dx.doi.org/10.1107/S0909049503024130.
51. **DeLano WL.** 2002. The PyMOL molecular graphics system, DeLano Scientific, San Carlos, CA.
52. **Pettersen EF, Goddard TD, Huang CC, Couch GS, Greenblatt DM, Meng EC, Ferrin TE.** 2004. UCSF Chimera—a visualization system for exploratory research and analysis. J Comput Chem **25:**1605–1612. http://dx.doi.org/10.1002/jcc.20084.
53. **Doria-Rose NA, Georgiev I, O'Dell S, Chuang GY, Staupe RP, McLellan JS, Gorman J, Pancera M, Bonsignori M, Haynes BF, Burton DR, Koff WC, Kwong PD, Mascola JR.** 2012. A short segment of the HIV-1 gp120 V1/V2 region is a major determinant of resistance to V1/V2 neutralizing antibodies. J Virol **86:**8319–8323. http://dx.doi.org/10.1128/JVI.00696-12.
54. **Kearse M, Moir R, Wilson A, Stones-Havas S, Cheung M, Sturrock S, Buxton S, Cooper A, Markowitz S, Duran C, Thierer T, Ashton B, Meintjes P, Drummond A.** 2012. Geneious Basic: an integrated and extendable desktop software platform for the organization and analysis of sequence data. Bioinformatics **28:**1647–1649. http://dx.doi.org/10.1093/bioinformatics/bts199.
55. **Crooks GE, Hon G, Chandonia JM, Brenner SE.** 2004. WebLogo: a sequence logo generator. Genome Res **14:**1188–1190. http://dx.doi.org/10.1101/gr.849004.
56. **Avery DT, Bryant VL, Ma CS, de Waal Malefyt R, Tangye SG.** 2008. IL-21-induced isotype switching to IgG and IgA by human naive B cells is differentially regulated by IL-4. J Immunol **181:**1767–1779. http://dx.doi.org/10.4049/jimmunol.181.3.1767.
57. **Zan H, Cerutti A, Dramitinos P, Schaffer A, Casali P.** 1998. CD40 engagement triggers switching to IgA1 and IgA2 in human B cells through induction of endogenous TGF-beta: evidence for TGF-beta but not IL-10-dependent direct S mu→S alpha and sequential S mu→S gamma, S gamma→S alpha DNA recombination. J Immunol **161:**5217–5225.
58. **Cerutti A, Zan H, Schaffer A, Bergsagel L, Harindranath N, Max EE, Casali P.** 1998. CD40 ligand and appropriate cytokines induce switching to IgG, IgA, and IgE and coordinated germinal center and plasmacytoid phenotypic differentiation in a human monoclonal IgM^+IgD^+ B cell line. J Immunol **160:**2145–2157.
59. **Sok D, van Gils MJ, Pauthner M, Julien JP, Saye-Francisco KL, Hsueh J, Briney B, Lee JH, Le KM, Lee PS, Hua Y, Seaman MS, Moore JP, Ward AB, Wilson IA, Sanders RW, Burton DR.** 2014. Recombinant HIV envelope trimer selects for quaternary-dependent antibodies targeting the trimer apex. Proc Natl Acad Sci U S A **111:**17624–17629. http://dx.doi.org/10.1073/pnas.1415789111.
60. **Pancera M, Lebowitz J, Schon A, Zhu P, Freire E, Kwong PD, Roux KH, Sodroski J, Wyatt R.** 2005. Soluble mimetics of human immunodeficiency virus type 1 viral spikes produced by replacement of the native trimerization domain with a heterologous trimerization motif: characterization and ligand binding analysis. J Virol **79:**9954–9969. http://dx.doi.org/10.1128/JVI.79.15.9954-9969.2005.
61. **Sharma SK, de Val N, Bale S, Guenaga J, Tran K, Feng Y, Dubrovskaya V, Ward AB, Wyatt RT.** 2015. Cleavage-independent HIV-1 Env trimers engineered as soluble native spike mimetics for vaccine design. Cell Rep **11:**539–550. http://dx.doi.org/10.1016/j.celrep.2015.03.047.
62. **McLellan JS, Pancera M, Carrico C, Gorman J, Julien JP, Khayat R, Louder R, Pejchal R, Sastry M, Dai K, O'Dell S, Patel N, Shahzad-ul-Hussan S, Yang Y, Zhang B, Zhou T, Zhu J, Boyington JC, Chuang GY, Diwanji D, Georgiev I, Kwon YD, Lee D, Louder MK, Moquin S, Schmidt SD, Yang ZY, Bonsignori M, Crump JA, Kapiga SH, Sam NE, Haynes BF, Burton DR, Koff WC, Walker LM, Phogat S, Wyatt R, Orwenyo J, Wang LX, Arthos J, Bewley CA, Mascola JR, Nabel GJ, Schief WR, Ward AB, Wilson IA, Kwong PD.** 2011. Structure of HIV-1 gp120 V1/V2 domain with broadly neutralizing antibody PG9. Nature **480:**336–343. http://dx.doi.org/10.1038/nature10696.
63. **Pancera M, Shahzad-Ul-Hussan S, Doria-Rose NA, McLellan JS, Bailer RT, Dai K, Loesgen S, Louder MK, Staupe RP, Yang Y, Zhang B, Parks R, Eudailey J, Lloyd KE, Blinn J, Alam SM, Haynes BF, Amin MN, Wang LX, Burton DR, Koff WC, Nabel GJ, Mascola JR, Bewley CA, Kwong PD.** 2013. Structural basis for diverse N-glycan recognition by HIV-1-neutralizing V1-V2-directed antibody PG16. Nat Struct Mol Biol **20:**804–813. http://dx.doi.org/10.1038/nsmb.2600.
64. **Bhiman JN, Anthony C, Doria-Rose NA, Karimanzira O, Schramm CA, Khoza T, Kitchin D, Botha G, Gorman J, Garrett NJ, Abdool-Karim SS, Shapiro L, Williamson C, Kwong PD, Mascola JR, Morris L, Moore PL.** 12 October 2015. Viral variants that initiate and drive maturation of V1V2-directed HIV-1 broadly neutralizing antibodies. Nat Med http://dx.doi.org/10.1038/nm.3963.
65. **McCoy LE, Falkowska E, Doores KJ, Le K, Sok D, van Gils MJ, Euler Z, Burger JA, Seaman MS, Sanders RW, Schuitemaker H, Poignard P, Wrin T, Burton DR.** 2015. Incomplete neutralization and deviation from sigmoidal neutralization curves for HIV broadly neutralizing monoclonal antibodies. PLoS Pathog **11:**e1005110. http://dx.doi.org/10.1371/journal.ppat.1005110.
66. **Liao HX, Lynch R, Zhou T, Gao F, Alam SM, Boyd SD, Fire AZ,**

Roskin KM, Schramm CA, Zhang Z, Zhu J, Shapiro L, NISC Comparative Sequencing Program, Mullikin JC, Gnanakaran S, Hraber P, Wiehe K, Kelsoe G, Yang G, Xia SM, Montefiori DC, Parks R, Lloyd KE, Scearce RM, Soderberg KA, Cohen M, Kamanga G, Louder MK, Tran LM, Chen Y, Cai F, Chen S, Moquin S, Du X, Joyce MG, Srivatsan S, Zhang B, Zheng A, Shaw GM, Hahn BH, Kepler TB, Korber BT, Kwong PD, Mascola JR, Haynes BF. 2013. Co-evolution of a broadly neutralizing HIV-1 antibody and founder virus. Nature **496:**469–476. http://dx.doi.org/10.1038/nature12053.

67. **Willis JR, Sapparapu G, Murrell S, Julien JP, Singh V, King HG, Xia Y, Pickens JA, LaBranche CC, Slaughter JC, Montefiori DC, Wilson IA, Meiler J, Crowe JE, Jr.** 2015. Redesigned HIV antibodies exhibit enhanced neutralizing potency and breadth. J Clin Invest **125:**2523–2531. http://dx.doi.org/10.1172/JCI80693.